Dynamic modeling of recirculating aquaculture systems with an integrated application of nonlinear model predictive control and moving horizon estimation

by

Sara Kamali

A thesis

presented to the University of Waterloo

in fulfillment of the

thesis requirement for the degree of

Master of Applied Science

in

Chemical Engineering

Waterloo, Ontario, Canada, 2022

AUTHOR'S DECLARATION

I hereby declare that I am the sole author of this thesis. This is a true copy of the thesis, including any required final revisions, as accepted by my examiners.

I understand that my thesis may be made electronically available to the public.

ABSTRACT

Growing concerns regarding the sustainability of the aquaculture industry has led to the development of recirculating aquaculture systems (RAS) where the addition of wastewater treatment units is accompanied by a reduction in water consumption and waste release. In this study, a mechanistic dynamic model of RAS was proposed and validated using experimental data available in the literature. Fish health is crucial to the profitability of an aquaculture facility; thus, fish performance and welfare measured in terms of growth and mortality were also incorporated within the proposed model. The model was then used to provide insights regarding the operation and management of RAS. According to the results of this analysis, continuous feeding was found to result in smaller fluctuations of waste product concentrations which is more desirable for the stability of wastewater treatment. Furthermore, under low rates of water exchange, addition of a denitrification unit to the RAS system would be necessary to avoid accumulation of nitrate.

The environment used for fish growth (i.e., rearing environment) plays a significant role in feed utilization as well as fish performance. Thus, water quality parameters such as concentration of oxygen and waste components should be constantly controlled in a way to meet fish requirements. To achieve this goal, a nonlinear model predictive control (NMPC) integrated with moving horizon estimation (MHE) was implemented in this study to control RAS environment. The performance of the proposed control scheme was evaluated under full and partial accessibility to the states in the presence of process uncertainty and measurement

noises. Assessment of the proposed controller was conducted by simulating the failure of unit or malfunction of a measurement device. In all scenarios, the proposed framework demonstrated the ability to maintain the water quality parameters close to target, indicating the promise of this control strategy in the closed-loop operation of RAS.

ACKNOWLEDGEMENTS

I would like to thank Prof. Luis A. Ricardez-Sandoval and Prof. Valerie C.A. Ward for giving me the opportunity to pursue my Masc. degree and being patient and attentive supervisors who guided me through this journey and improved my performance through careful revisions and advises.

I would like to thank my examining committee Prof. Abukhdeir and Prof. Meunier for taking the time and efforts to review my thesis and providing valuable feedback and comments to improve my thesis.

I would like to thank my parents for believing me and being there for me through difficulties and trying to teach me how to be strong when it was so hard.

I'm especially grateful to my lovely family in Iran who supported me with their trust and unconditional love.

And to all my wonderful friends who helped me in this journey: Daniela, Thiago, Camila, Mahshad, Oscar, Gabriel, and David.

Finally, I want to thank the financial assistance provided by the Natural Sciences and Engineering Research Council of Canada (NSERC).

DEDICATION

Dedicated to the best parents I could ever have: Azam and Javad

TABLE OF CONTENTS

LIST OF FIGURES

LIST OF TABLES

LIST OF ABBREVIATIONS

AOB	Ammonia oxidizing bacteria
AC	Arrival cost
ASM	Activated sludge model
ASM1	Activated sludge model No. 1
ASM1-2N	Extension of activated sludge model No. 1 with two-step nitrification and denitrification processes
0DBFM	Zero-dimensional biofilm model
BOD_5	Five-day biochemical oxygen demand
BOD_{20}	Twenty-day biochemical oxygen demand
COD	Chemical oxygen demand
DO	Dissolved oxygen
het	Heterotrophic bacteria
MBBR	Moving bed bioreactor
MHE	Moving horizon estimation
NMPC	Nonlinear model predictive control
NOB	Nitrite oxidizing bacteria
PI	Proportional–Integral controller
PID	Proportional–Integral–Derivative controller
RAS	Recirculating aquaculture system
SSE	Sum of squared errors

NOMENCLATURE

a	Fraction of the food assimilated that is used for feeding catabolism
A	Un-ionized ammonia concentration in the fish tank (mg/L)
A_{crit}	Critical unionized ammonia concentration (mg/L)
A_{max}	Maximum unionized ammonia concentration (mg/L)
b_{AOB}	Decay coefficient for AOB bacteria (day^{-1})
b_{NOB}	Decay coefficient for NOB bacteria (day^{-1})
b_H	Decay coefficient for heterotrophic biomass (day^{-1})
c	Allometric scaling factor
C	Length of control horizon
DO_{crit}	Critical dissolved oxygen (mg/L)
DO_{min}	Minimum dissolved oxygen (mg/L)
f	Food availability
f_P	Fraction of biomass leading to particulate products (dimensionless)
F	Process model
G	Inequality constraints
h	Coefficient of food consumption ($g^{1-m}day^{-1}$)
H	Measurement model function
i	Index of time interval within the prediction horizon
i_{CV}	Particulate COD/volatile suspended solids (dimensionless)
i_{XB}	Mass of nitrogen per mass of COD in biomass ($g\ N\ /\ g\ COD$)
i_{XP}	Mass of nitrogen per mass of COD in products from biomass ($g\ N\ /\ g\ COD$)
j	Index of time interval within the estimation horizon
J	Constant to describe temperature on catabolism ($°C^{-1}$)

k	Index of the current time interval
K	Catabolism coefficient ($g^{1-m}day^{-1}$)
K_a	Ammonification rate ($m^3(gCODday)^{-1}$)
k_{attach}	Attachment rate constant ($m^3g^{-1}day^{-1}$)
k_{detach}	Detachment rate constant ($m^3g^{-1}day^{-1}$)
$K_{L,CO2}$	Mass transfer coefficient for carbon dioxide (day^{-1})
$K_{L,O2}$	Mass transfer coefficient for oxygen (day^{-1})
k_{min}	Coefficient of fasting catabolism ($g^{1-n}day^{-1}$)
K_{NH}	Half-saturation (auto. growth) ($(gNH_3 - Nm^{-3}$)
$K_{NH,I}$	Ammonia inhibition of nitrite oxidation ($gNH_4 - Nm^{-3}$)
K_{OA}	Half-saturation (auto. oxygen) ($(gO_2m^{-3}$)
K_{OH}	Half-saturation (hetero. oxygen) ($(gNH_3 - Nm^{-3}$)
K_{NOx}	Half-saturation (nitrite and nitrate) ($gNO_3 - Nm^{-3}$)
K_S	Half-saturation (hetero. growth) ($gCODm^{-3}$)
K_X	Half-saturation (Hydrolysis)
m	Exponent of body weight for net anabolism
M	Fish biomass (kg)
M_u	Natural mortality rate at unit weight
$m_{O2,FT}$	Oxygen flow rate to the fish tank (kg/day)
$m_{air,MBBR}$	Air flow rate to MBBR (m^3/day)
n	Exponent of body weight for fasting catabolism
N	Length of estimation horizon
NF	Number of fish
P	Length of prediction horizon
$pK_a{}^0$	Ionization constant at 25℃ for the ammonium ion

N_o	Initial number of fish
$\boldsymbol{Q}$	Covariance matrix of process uncertainties
$\boldsymbol{Q_{CV}}$	Weights on the controlled variables
$\boldsymbol{Q_{MV}}$	Weights on the manipulated variables
Q_{BR}	Flow to the bioreactor (m^3)
Q_{tank}	Flow to the fish tank (m^3)
$Q_{make-up}$	Make-up water flow rate to the fish tank (m^3/day)
$r_{0D\ BFM_i}$	rate of change of component i
$\boldsymbol{R}$	Covariance matrix of measurement noises
s_k	Salinity of water
S_{Alk}	Alkalinity $(mol\ L^{-3})$
S_{CO2}	Carbon dioxide $(g\ COD\ m^{-3})$
$S_{CO2,sat}$	Carbon dioxide saturation concentration in the water (mg/L)
S_I	Soluble inert organic matter $(g\ COD\ m^{-3})$
S_{ND}	Soluble biodegradable organic nitrogen $(g\ N\ m^{-3})$
S_{NH}	Ammonia nitrogen $(g\ N\ m^{-3})$
S_{NO2}	Nitrite nitrogen $(g\ N\ m^{-3})$
S_{NO3}	Nitrate nitrogen $(g\ N\ m^{-3})$
S_O	Oxygen $(g\ COD\ m^{-3})$
$S_{O2,sat}$	Oxygen saturation concentration in the water (mg/L)
S_S	Readily biodegradable substrate $(g\ COD\ m^{-3})$
t	Time (day)
T	Temperature (°C)
T_{min}	Lower limit for temperature (°C)
T_{max}	Upper limit for temperature (°C)

T_{opt}	Optimal temperature (℃)
UL_{NH3}	Upper limit on total ammonia concentration (mg/L)
UL_{NO3}	Upper limit on nitrate concentration (mg/L)
v_j	Measurement noise at the jth time interval within time horizon N
V_{BR}	Bioreactor volume (m^3)
V_{tank}	Fish tank volume (m^3)
w_j	Process uncertainty at the jth time interval within time horizon N
W	Body weight (g)
x	State of the system
$x_{nominal}$	Nominal steady-state value of the states
x'_i	State of the system at the ith time interval within time horizon P
$\widehat{x_k}$	Estimated state obtained from MHE at the current time interval k
x^l, x^u	Bounds on the states
X_{AOB}^B	AOB biomass in the biofilm ($g\ COD\ m^{-3}$)
X_{AOB}^S	AOB biomass in suspension ($g\ COD\ m^{-3}$)
X_{NOB}^B	NOB biomass in the suspension ($g\ COD\ m^{-3}$)
X_{NOB}^S	NOB biomass in suspension ($g\ COD\ m^{-3}$)
X_H^B	Heterotrophic biomass in the biofilm ($g\ COD\ m^{-3}$)
X_H^S	Heterotrophic biomass in suspension ($g\ COD\ m^{-3}$)
X_I^B	Particulate inert organic matter in the biofilm ($g\ COD\ m^{-3}$)
X_I^S	Particulate inert organic matter in suspension ($g\ COD\ m^{-3}$)
X_{ND}^B	Particulate biodegradable organic nitrogen in the biofilm ($g\ N\ m^{-3}$)
X_{ND}^S	Particulate biodegradable organic nitrogen in suspension ($g\ N\ m^{-3}$)
X_P^B	Particulate products arising from biomass decay in the biofilm ($g\ COD\ m^{-3}$)
X_P^S	Particulate products arising from biomass decay in suspension ($g\ COD\ m^{-3}$)

X_S^B	Slowly biodegradable substrate in the biofilm ($g\ COD\ m^{-3}$)
X_S^S	Slowly biodegradable substrate in suspension ($g\ COD\ m^{-3}$)
y_j	Measurement of the system at the jth time interval within time horizon N
y'_i	Output of the system at the ith time interval within time horizon P
Y_{AOB}	AOB yield ($g\ COD\ /\ g\ N$)
Y_{NOB}	NOB yield ($g\ COD\ /\ g\ N$)
Y_H	Heterotrophic yield ($g\ COD\ /\ g\ N$)
ε_{loss}	Feed loss fraction
η_g	Anoxic growth rate correction factor (dimensionless)
η_h	Anoxic hydrolysis rate correction factor (dimensionless)
η_{NO3}	Anoxic growth rate correction factor S_{NO3}(dimensionless)
μ_H	Maximum heterotrophic growth rate (day^{-1})
μ_{NB}	Maximum NOB growth rate (day^{-1})
μ_{NS}	Maximum AOB growth rate (day^{-1})
τ	Feed residence time (day)
φ_{k-N}	AC estimated at time $k-N$

Chapter 1

Introduction

Aquaculture is the practice of farming fish, crustaceans, molluscs, algae and other valuable organisms in water. As of 2018, worldwide aquaculture formed 46 percent of total production (aquaculture and capture) and reached a high record of 82.1 million tonnes (FAO, 2020). Aquaculture is primarily conducted in floating cages in marine or fresh waters or in flow-through systems on land. However, the release of untreated wastewater from cages stocked with high fish densities and the high-water usage in land-based flow-through systems have raised concerns over the long-term sustainability of these systems. These ecological concerns can be addressed by using land based recirculating aquaculture systems (RAS). In these systems, the addition of a wastewater treatment section allows to recirculate 90–99% of the water used in the rearing tanks (i.e., the tanks used for fish growth) thus reducing water consumption (Badiola et al., 2012; Martins et al., 2010; Zhang et al., 2011). Moreover, recirculated systems using a high recirculation rate can reduce the fish waste discharged into bodies of water by up to 90% compared to sea cages as the water treatment process removes fish waste products and collects them into a high concentration sludge stream that can be dried and used for biogas production or as fish manure (Vielma et al., 2021). Finally, aquaculture systems that are open to the environment like flow-through systems or sea cages are subject to the introduction of viruses, bacteria, or parasites from the water or from adjacent wild-life populations, respectively (FAO, 2020). A recent example estimates the losses due to

hepatopancreatic necrosis outbreak in Thailand at over 11 billion USD (Shinn et al., 2018). RAS systems provide the highest level of biosecurity (FAO, 2020)

Note that the intense reuse of water and low rate of water exchange in RAS can also lead to the accumulation of toxic waste in water (Vielma et al., 2021). To this regard, the quality of the water in RAS should be carefully monitored and the water quality parameters such as dissolved oxygen, temperature, and waste concentrations must be maintained within acceptable ranges such that fish experience less stress, achieve lower mortalities, and obtain higher growth rate (Fowler et al., 1994). To this aim, it is of primary importance to continuously remove the waste that is produced through fish excretion and uneaten food and adjust the oxygen and carbon dioxide content of water (i.e., add oxygen and remove carbon dioxide). This being said, in RAS, the fish tank effluents pass through a mechanical filtration where solid wastes primarily resulting from feces production and uneaten food are eliminated. The remaining small particles and dissolved waste components are then passed through reactors where biological reactions performed by microorganism transform toxic components such as ammonia to less toxic compounds such as nitrate (a process known as nitrification, Rusten et al., 2006). An aerator for oxygen addition and a stripping unit for carbon dioxide removal are then used to adjust the oxygen and carbon dioxide content of water. Other units such as denitrification reactors (used for conversion of nitrate to nitrogen gas), ultraviolet light or ozone disinfection (for the removal of pathogens and unwanted organisms), pH regulation, heat exchanging, etc. can then be added to RAS if needed (Bregnballe et al., 2010).

RAS is a relatively new technology (Ahmad et al., 2021); thus further work is required to provide insights into operation and performance of these systems. In contrast to experimental

development, which is often time-consuming and expensive; the application of mathematical modeling allows to carry out experiments in a simulation environment that can save time and money in the optimal design and operation of dynamic systems (Rafiei & Ricardez-Sandoval, 2020a; Zhou et al., 2021). Having access to a RAS model can also be used to determine the most suitable control systems for their operation, determine the sizing of the major units in a RAS, and specify the sensors that may be needed to adequately monitor the process during operation. In this regard, Losordo and Hobbs, (2000) and Tidwell, (2012) proposed stationary models with the purpose of design and sizing of RAS. Wik et al., (2009) and Karimanzira et al., (2016) focused on dynamic modeling of RAS based on the component mass balances and waste characterization to estimate waste production and predict the transient behavior of RAS that can be used to analyze the operation of this system under different scenarios. In order to understand how the rearing environment would impact fish growth and survival, the proposed model should account for the inherent interactions between the fish performance and the quality of water in the system. However, the effect of water quality parameters such as oxygen concentration or temperature on fish have not been investigated in the literature. Therefore, incorporation of a fish growth model within RAS equations that reflects the effect of environment on fish well-being is critical to assist the farmers in operating RAS based on fish needs.

As mentioned earlier, one of the applications of the dynamic modeling of RAS is the feedback analysis of the system (design and implementation of controllers) which aims to maintain the quality of the water within the range compatible with fish needs (Fowler et al., 1994). In this regard, there have been several efforts in the literature to control the operation of RAS. Most

of the studies in this area have implemented fuzzy logic and decentralized linear controllers such as PI (proportional-integral) or PID (proportional – integral – derivative) to control RAS (Farghally et al., 2014; Wik et al., 2009). However, the control schemes employed in those studies are mostly single input single output (SISO) control. However, RAS is a highly interactive system with multiple inputs and multiple outputs (MIMO) that should be controlled simultaneously to avoid major losses in the performance of the system. To account for the nonlinear and highly interactive behavior of RAS as well as the water quality constraints (e.g., maximum allowed concentration of toxic components), the application of advanced model-based MIMO (multiple input- multiple output) controllers is needed. Nonlinear model predictive controller (NMPC) is an advanced model-based controller that computes a trajectory of control actions such that the predicted outputs achieve their corresponding setpoints within a finite time horizon. Accurate initialization of the states in NMPC is crucial for proper performance of NMPC; however, online measurements for all of the states is not often available (due to high cost and low reliability of the measurement devices). A state estimator is thus needed to estimate the unmeasurable states necessary for NMPC implementation. This estimator employs the available measurement of the system together with a process model to estimate the unmeasurable states. To the author's knowledge, a study involving state estimation and advanced model-based control in RAS is not currently available. Among all the different estimators proposed in the literature, moving horizon estimation (MHE) is an attractive choice for RAS application due to the ability to handle complex behavior of RAS as well as taking into account the biological constraints in the system (Alexander et al., 2020). To

date, the application of a MHE-NMPC framework for closed-loop operation of RAS has not been explored, representing another gap in the existing literature for RAS.

1.1 Research objectives

The purpose of this thesis is to provide new insights on the mathematical modeling of RAS and propose a new model-based optimization framework for the optimal operation of RAS in closed-loop. To pursue these objectives, the current study focuses on the following research objectives:

- Develop a dynamic model for the RAS that can be integrated with a fish growth model capable of capturing the effects of rearing environment on fish growth.
- Evaluate the effects of water quality parameters (e.g. temperature, oxygen concentration) and management strategies (e.g. make-up flow rate to fish biomass ratio, feeding regime) on fish performance.
- Analyze the closed loop operation of RAS through implementation of a nonlinear model predictive controller (NMPC) integrated with the moving horizon estimation (MHE).

The integrated dynamic RAS model developed in this study can estimate the produced waste in the fish tanks, which is key in determining the quality of water in the system as well as the waste load to the treatment section. Moreover, the fish growth model incorporated in the system can be used to predict the fish growth, given the conditions and quality of water in the rearing environment. The proposed closed loop framework (involving state estimation methods with model-based control schemes) can be applied to control RAS in the presence of process and measurement noises and even under partial accessibility to the states (due to limitations in

the measurement devices). Moreover, the proposed control scheme can also be used in RAS to keep the rearing environment compatible with fish requirements under common disruption occurring in the actual operation of the system such as failure of an operating unit or malfunction of a sensor. Insights from the closed-loop operation in RAS would be key to further advance the technological development and commercialization of these emerging systems.

1.2 Structure of the thesis

This thesis is organized as follows:

Chapter 2 introduces RAS and the key units involved in the operation of these systems. A literature review on the current state-of-the-art of modeling of RAS is presented next in this chapter followed by a thorough review of literature in closed-loop operation of RAS. The gaps in the literature that motivate this research are explicitly discussed in this chapter.

Chapter 3 introduces the proposed integrated dynamic RAS and fish growth model. Validation of the proposed model using experimental data available in the literature is explicitly discussed in this chapter as well. Fish growth under different water quality parameters and management strategies is assessed next in this chapter and the results of this analysis are discussed in detail at the end of this chapter.

Chapter 4 focuses on implementation of NMPC and MHE in RAS with the aim of improving the closed-loop performance of this system. Multiple scenarios in the operation of RAS such as failure of a unit or malfunction of a sensor are considered to further analyze the closed-loop performance of the system.

Chapter 5 presents the concluding remarks and contributions achieved by this study. This chapter also provides recommendations for future works.

Chapter 2

Literature Review

This chapter presents the current state-of-the-art in modeling and closed-loop operation of recirculating aquaculture systems (RAS) to clarify the gaps motivating this work and outline the contributions made to this area of research. To this aim, Section 2.1 provides a conceptual framework and background for RAS and illustrates the main units involved in the operation of these systems. Section 2.2 discusses the existing studies in the modeling of RAS whereas the current state-of-the-art in closed-loop operation of RAS, and the implementation of different control strategies, are explained in Section 2.3. A summary of this chapter is presented at the end.

2.1 Recirculating aquaculture systems (RAS)

Aquaculture is defined as the farming of aquatic animals and plants such as fish, shrimps, algae etc. (Sapkota et al., 2008). The growing demand for fish has led to a significant growth in the contribution of aquaculture to the global fish production. As of 2018, fish[*] aquaculture constitutes 46% of the total production (aquaculture + capture) and 52% of fish for human consumption with an average production of 82.1 million tonnes per year (FAO, 2020).

Culture systems for aquaculture can be classified as open systems (e.g., cage, net pens), semi-closed systems (e.g., raceways and ponds), and closed systems (e.g., recirculating aquaculture systems). This classification is based on stocking densities (i.e., how densely the animals are

[*] Here the term "fish" indicates fish, crustaceans, molluscs and other aquatic animals, but excludes aquatic mammals, reptiles, seaweeds and other aquatic plants

stocked into the system) and the human intervention to control the system (e.g., control of temperature, oxygen, waste removal) (Ahmad et al., 2021; Tidwell, 2012). Open systems are normally natural bodies of water used for commercial production. Note that these systems heavily rely on the natural processes for waste removal, providing sufficient oxygen, and maintaining adequate temperatures; for example, oxygen is provided through natural processes such as diffusion or photosynthesis of algal communities in these systems. Semi-closed systems are manmade production units that still rely on nature to maintain the quality of water within acceptable levels; however, they provide better control over water depth or water replacement in the system as well as elimination of competitors and predators (Tidwell, 2012). These systems also known as once-through or flow-through systems, consume a lot of water since the water passes through them only once and then discharges out (Ahmad et al., 2021).

Recirculating aquaculture (RAS) is a closed system that aims to address the problems associated with the systems discussed above. Addition of a wastewater treatment in RAS that allows for 90–99% of the water to be recirculated within the system can reduce the water consumption and waste discharge to the environment (Badiola et al., 2012; Martins et al., 2010; Wik et al., 2009; Zhang et al., 2011). Constant monitoring and control over the water quality parameters (such as temperature, oxygen) as well as reduction of risks associated with pathogens and diseases are key features in a typical RAS system (Wik et al., 2009). Moreover, proximity to the markets which is accompanied by a reduction in carbon dioxide emissions associated with food transport, are additional features that make RAS an attractive option for fish growth and production (Martins et al., 2010).

The RAS sector is growing rapidly, e.g., the application of these environmentally friendly systems for the production of fingerling and grow-out species is increasing across the world (Vielma et al., 2021). As of 2020, Norway is a leader with 23 land-based salmon or large rainbow trout RAS projects followed by the United States and China with 17 and 8, respectively (Vielma et al., 2021). Japan and Canada are ranked 4th and 5th, respectively with 6 and 5 large RAS projects (Vielma et al., 2021). Despite its sustainability and the increasing number of RAS projects worldwide, RAS still makes a small contribution to total fish production due to high operating and capital costs (Chen et al., 1993; Martins et al., 2010). Higher stocking densities and production rates are often required to make RAS economically attractive (Martins et al., 2010). Despite the challenges discussed above; RAS is still a promising technology that can be used in sustainable production of aquatic animals.

As mentioned earlier, the high degree of water recirculation as well as low rate of daily water exchange in RAS can lead to the accumulation of toxic wastes in water (Vielma et al., 2021). In this regard, the quality of the water in RAS should be carefully monitored to ensure that the water quality parameters such as dissolved oxygen, temperature, and waste concentrations are maintained within acceptable ranges for highest growth and maximum fish survival. To this aim, it is of primary importance to adjust the oxygen and carbon dioxide content within the water (addition of oxygen and remove carbon dioxide) and remove the produced waste as a result of feces production and uneaten food to ensure fish welfare (in terms of fish growth). Fig. 2.1 shows the main units in the operation of RAS that are necessary to keep the quality of water compatible with fish needs. According to this figure, the fish tank effluents pass through a solid capture unit where the solid wastes primarily resulting from feces production and uneaten food

are eliminated. The remaining small particles and dissolved waste components are then passed through a biological treatment where biological reactions performed by microorganisms transform toxic components such as ammonia to less toxic compounds such as nitrate (Rusten et al., 2006). An aerator for oxygen addition and a stripping unit for carbon dioxide removal are then used to adjust the oxygen and carbon dioxide content of water. Other units such as denitrification reactors (used for conversion of nitrate to nitrogen gas), ultraviolet light or ozone disinfection (for the removal of pathogens and unwanted organisms), pH regulation, heat exchangers, etc. can then be added to make RAS an efficient operation (Bregnballe et al., 2010). A detailed explanation of the main units involved in a typical RAS is provided next.

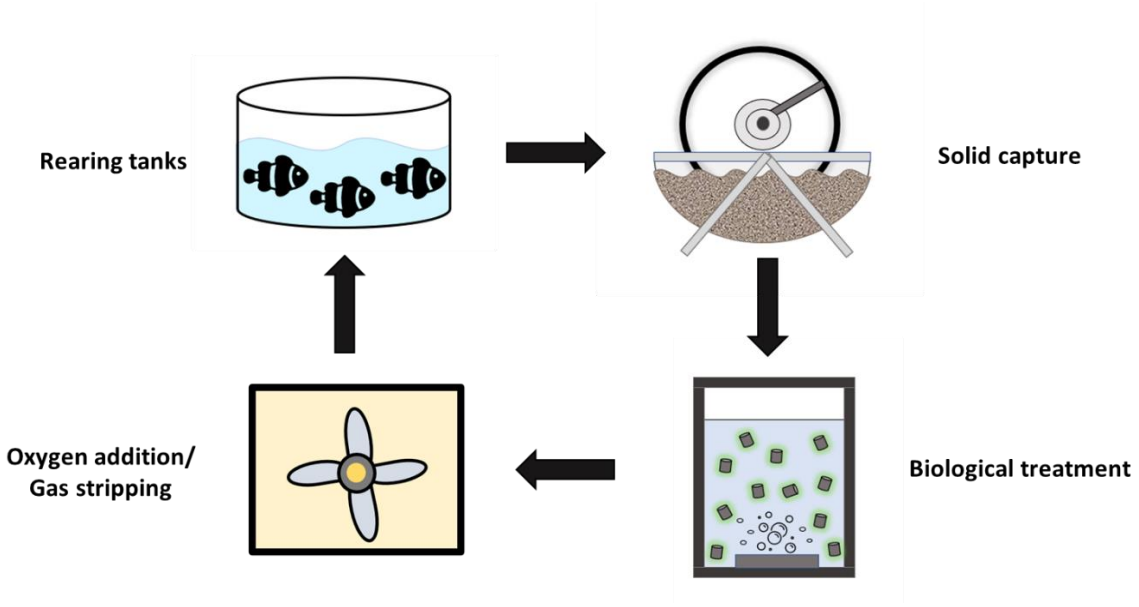

Fig. 2.1 A simple schematic of main units in RAS.

- **Rearing tanks (fish tanks)**

Fish rearing tank is a key unit within the fish farms, not only because they are the environment used for fish culture and growth, but also because they are the source of water use and waste production (Davidson & Summerfelt, 2004). As a result of feeding and fish excretion, the quality of water in the fish tank deteriorates over time and thus waste management becomes of high priority where the waste produced in the fish tanks should be removed rapidly and effectively to ensure fill welfare. Moreover, the tank's design (i.e., shape and size), depth of water, and self-cleaning ability can affect the performance and well-being of the fish significantly. Hence, they need to be chosen according to the fish requirements (Bregnballe et al., 2010). For example, for bottom dwelling fish (fish stay in the bottom of the tank), a large surface area is important whereas the depth and speed of water current is less significant. Tank design can also significantly affect the capital and operating costs (Bregnballe et al., 2010; Ross & Watten, 1998; Timmons et al., 2002). Large circular tanks (diameters > 10m) are an attractive choice for fish culture due to rapid flushing of settleable solids, simple maintenance, and uniform water quality (Timmons et al., 2002).

- **Solid capture**

Solid wastes produced as a result of feces production or uneaten food form a high percentage of total waste released by fish in aquaculture (Bureau & Hua, 2010). These solids are composed of particles with different sizes (Timmons et al., 2002), however, 95% of these particles have a diameter less than 20 microns (Chen et al., 1993). To filter the water, a microscreen with a mesh size of typically 40 to 100 micron is of interest in almost all recirculated fish farms. Drum

filter is the most popular microscreen filter in mechanical filtration and solid removal in RAS (Bregnballe et al., 2010).

- **Biological treatment**

Biological treatment systems use microorganisms for waste treatment and removal of unwanted components. These systems can be divided into suspended and attached growth systems. In a suspended (dispersed) system, microorganisms are suspended in the bulk whereas in attached growth systems, microorganisms grow on a support medium (carrier) and form a layer called biofilm (Sehar & Naz, 2016). Construction of compact reactors and easier separation of the biomass from the treated effluent (Bassin et al., 2016) have led to the selection of attached biomass system over suspended systems.

There are many different biofilm systems in use (attached growth); such as trickling filters, rotating biological contactors (RBC), fixed media submerged biofilters, granular media biofilters, fluidised bed reactors, moving bed biofilm reactor (MBBR), etc. (Kawan et al., 2016). In recent years, application of MBBR has become more common in aquaculture (Fernandes et al., 2017). MBBR have high specific surface area and biomass density and require low maintenance (Kawan et al., 2016). Moreover, MBBR are more appealing than fixed biomass systems such as trickling filters and submerged biofilters, since they show no clogging problems and have lower head loss (Andreottola et al., 2000).

MBBR is a completely mixed reactor with carriers lighter (less dense) than water that are in constant movement. Depending on the type of the reactor, i.e., aerated or non aerated, this movement can be achieved through aeration and mechanical stirring, respectively (Kermani et

al., 2008). In MBBR, removal is mostly done through the biomass attached on the carriers; nevertheless, the exchange of biomass between bulk and biofilm can change the contribution of each compartment (bulk or biofilm) in total waste removal (Piculell et al., 2013).

MBBR are mainly used for nitrification in aquaculture applications, which is a biological process that transforms ammonia into a less toxic component such as nitrate (Rusten et al., 2006). Ammonia (NH_3) is released from the fish gills as a product of protein catabolism and exists in equilibrium with its much less toxic ionized form, i.e., ammonium (NH_4^+). The sum of the unionized and ionized forms is referred to as the total ammonia nitrogen (TAN). Temperature, pH, and salinity affect the proportion of $NH_3/NH_4{}^+$ (Fivelstad et al., 1995; Timmons et al., 2002; Wik et al., 2009). Nitrification is a two-step process; in the first step, ammonia is converted into nitrite by ammonia oxidizing bacteria (AOB) whereas in the second step, the nitrite produced in the previous step is oxidized by nitrite oxidizing bacteria (NOB) to nitrate (Ostace et al., 2011; Pedersen, 2018). In contrast to nitrite and ammonia, nitrate toxicity is low due to the low permeability of nitrate through the fish gill (Camargo et al., 2005). However, high nitrate concentrations can negatively affect fish growth (van Rijn et al., 2006) and transform haemoglobin into methaemoglobin, i.e., the form that does not carry oxygen and thus should be avoided (Camargo et al., 2005). To avoid high concentration of nitrate, the addition of denitrification units is recommended. Denitrification is a process in which, oxidized inorganic nitrogen compounds such as nitrite and nitrate are reduced to gaseous forms of nitrogen such as nitrogen gas. However, due to financial concerns, the application of denitrification in commercial RAS is currently limited (van Rijn et al., 2006).

- **Oxygen addition/gas stripping**

Before the water returns to the fish tanks, the oxygen content of the water as well as the concentration of accumulated gases (such as carbon dioxide) caused by fish and microorganisms respiration must be regulated (Bregnballe et al., 2010). Pumping the air into the water, a process known as aeration, is a common method to add oxygen to the water. The turbulence caused by the aeration and the contact between water and the air can remove the gases in the water such as carbon dioxide. The driving force for gas exchange between the water and the air is the saturation level of the oxygen in the water with the equilibrium value of 100% saturation. To ensure sufficient availability of oxygen in water, a high saturation level is preferred which can be achieved through addition of pure oxygen (Bregnballe et al., 2010). Sources of pure oxygen in aquaculture often involve high pressure oxygen gas, liquid oxygen, and on-site oxygen generations. As emergency backup, at least two of these sources are available in most facilities. (Timmons et al., 2002). High pressure oxygen gas is normally used only for emergencies because of their high cost and limited capacity. Liquid oxygen is very reliable since it is expected to maintain the oxygen for at least 30 days; however, oxygen is a very strong oxidizing agent and special care should be taken for handling of this species (Timmons et al., 2002).

Pressure swing adsorption (PSA) and vacuum swing adsorption (VSA) can be used to generate oxygen on-site through a molecular sieve used to selectively adsorb nitrogen form the air and produce oxygen-enriched gas. However, despite the reliability and low maintenance requirements of these oxygen generators, they are expensive and also require electrical power;

thus, other sources of oxygen should be available as backups in the case of power failure (Timmons et al., 2002).

To provide a good rearing environment capable of keeping fish healthy, it is key to understand how fish and RAS system respond to different conditions. For example, how oxygen requirements of the fish vary during the feeding period or how temperature variations affect the fish growth. Moreover, estimation of the waste produced through fish excretion and uneaten feed is fundamental since the produced waste (if not removed properly) can significantly impact fish health. Nevertheless, RAS is a recent innovation and is still in its infancy (Ahmad et al., 2021); thus, further research is required for better understanding of these systems. Pilot and full-scale experimentation of RAS can provide useful information about these system; however, in addition to the cost and complexity of performing experimental works, RAS has slow dynamics i.e., time characteristics of RAS due to presence of fish and microorganism can vary up to several months (Wik et al., 2009). However, mathematical models describing the operation of these systems can be used as an alternative approach for experimentation in a virtual environment. These models can help farmers and aquaculturists to estimate waste production, predict fish growth under the provided rearing environment, and analyze the effect of different RAS design and configuration on fish performance and waste removal. Moreover, these models can further be used in developing control schemes that can maintain the RAS system within the acceptable range for fish growth. The next section reviews the current state-of-the-art in modeling of RAS.

2.2 Modeling of RAS

A RAS model can be constructed using a modular approach, i.e., RAS system can be divided into smaller units (fish tanks, mechanical treatment, biological reactors, etc.) and each unit is modeled separately. All the units are then integrated through material/energy streams and the entire RAS model is created. In this approach, a unit can easily be added, or substituted with an existing unit; thus, providing flexibility in terms of RAS design and modeling. The importance of this RAS model to conduct experiments on RAS in a simulated environment for better understanding, design, and further feedback analysis of the system has motivated the development of several models for these systems. Tidwell, (2012) focused on providing a better idea in designing RAS; in that study, the authors developed a model to calculate the required volume, depth, and the number of the fish tanks based on fish growth rate and the allowable fish biomass stocking densities in each tank. That study also determined the required flow rate within the system through stationary mass balances for oxygen, total ammonia, carbon dioxide, suspended solids, and nitrate such that all the water quality parameters considered in that model meet the fish requirements. Losordo & Hobbs, (2000) developed a spreadsheet based on a set of stationary mass balance equations for the waste metabolites produced and the oxygen consumed within the system. The proposed mass balances were used to estimate the required flow rates within RAS as well as the recycle and make-up water flow rate. The spreadsheet proposed in that work is capable of estimating the required biofilter volume and cross-sectional (top) surface area for the given biofilter shape, depth and specific surface area of the biofilter media. The studies conducted by Losordo & Hobbs, (2000) and Tidwell, (2012) mostly focused on the design and sizing of RAS through stationary models; however, to understand system's

dynamics and develop control strategies, addition of a dynamic model is of great importance. Wik et al., (2009) built a dynamic model based on mass component balances and waste characterization for RAS. The proposed dynamic model was used to develop a simulator within the MATLAB environment. This simulator can be applied to any combination of fish, feed and treatment provided the required data for the plant is given and used to analyze, predict and explain RAS performance. Moreover, closed-loop operation of RAS through implementation of controllers to this simulator is also possible. That dynamic model did not consider the inherent interactions between the fish growth and the performance of the treatment section thus neglecting the effects of water quality parameters that would influence fish growth and well-being. Following the same ideas and principles considered by Wik et al., (2009), Karimanzira et al., (2016) presented a dynamic model for a RAS coupled with a greenhouse hydroponic system (GHS). The proposed model was implemented in VBA Excel and used to describe the behaviour of Nile tilapia and tomato production. Despite the capability of model in simulating the system under different scenarios, the fish response to RAS management strategies such as degree of water recirculation or variations in the operating conditions of the system were not explicitly considered in that study.

In contrast to the studies mentioned above that considered modeling of the entire RAS, Zhou et al., (2021) and Zhou et al., (2022) only focused on modeling the dissolved oxygen content (DO) in RAS. Zhou et al., (2021) obtained an empirical model between DO and the aerator flow rate through open-loop experiments whereas (Zhou et al., 2022) developed a mechanistic model for DO by taking into account the main factors influencing the DO content such as circulating water flow, mechanical aeration, surface reaeration, and respiration. The proposed models

were mainly developed for DO control in RAS through implementation of adaptive PID controllers (See Section 2.3). Note that despite the high accuracy of these model to predict DO content of water, their application is only limited to prediction of oxygen concentration in RAS and they cannot be used for other purposes such as estimation of fish growth or waste production, which are crucial for design and operation of RAS. The present study aims to address the gaps in the modeling of RAS. This model will be discussed in detail in chapter 3.

2.3 Closed-loop operation of RAS

The most important parameters to control in RAS are related to the quality of the water in the fish tanks, i.e., temperature, dissolved oxygen (DO), pH, salinity, alkalinity, concentration of ammonia, nitrite, nitrate, suspended solids, and biochemical oxygen demand (BOD) (Fowler et al., 1994). These parameters can affect fish well-being, feed utilization, and growth rates; thus, they needed to be carefully monitored and controlled (Fowler et al., 1994). To this aim, there have been several attempts in the literature to control one or several water quality parameters in RAS. Wik et al., (2009) implemented multiple PI controllers for oxygen control (DO) through the manipulation of liquid oxygen or aeration, and denitrification control by the addition of an external carbon (this external carbon which could be derived from fermented sludge is added to the system when there is not sufficient biodegradable substrate in the fish tanks effluents to denitrify all the nitrate produced in the nitrification). The experiment was conducted for 100 tonnes of annual production of rainbow trout with 14 parallel rearing tanks. According to the results, in contrast to DO control, nitrate control in RAS is troublesome because of the stiff nature of the system due to different time scales (i.e., slow bacterial growth in contrast to fast behavior of solutes in the biofilm). Also, recirculation effects make the nitrate control to cause

large fluctuations in the system. However, PI feedback controller behaved properly in the absence of water recirculation.

Fuzzy logic control (FLC) is a popular choice in closed-loop operation of RAS due to easy implementation, the ability to handle nonlinear complex systems, and that no process model is needed to tune the controller (Farghally et al., 2014). Previous studies in this area have either used a single FLC or combined it with other control frameworks (Farghally et al., 2014; Jie et al., 2019) to improve the closed-loop performance of RAS. The basis of FLC is a fuzzy set that describes the membership of an object by a number between zero and one and then emulate human expert knowledge and experience to process information and make decisions (Lee et al., 2000).

In this regard, Farghally et al., (2014) controlled the water temperature using geothermal heat in a catfish RAS system using three different control schemes: a PI controller, a fuzzy logic controller, and a fuzzy-PID controller; in this work, the PID tuning parameters were determined through the membership function of the inputs (error, change of error), and the outputs (PID tuning parameters) of the FLC. The results of this study under variability in water temperature over a day showed that the fuzzy controller performed the best in terms of setpoint tracking and minimum error signal while controlling the water temperature in the RAS. Jie et al., (2019) aimed to control the DO using three different strategies: a conventional PID controller, a fuzzy PID control, and a fuzzy PID control combined with the gray prediction model. The fuzzy controller takes the error between the DO and the given setpoint as well as the change of the error as the input of the FLC. After fuzzification, three PID parameters are adjusted online based on fuzzy rule base. Then the PID controller adjusts the control variable to maintain the DO at

the setpoint. The last methodology considered in that work was proposed to overcome the large hysteresis of DO control in RAS through addition of a gray prediction model to the fuzzy logic control. The gray prediction model predicts the change of DO based on the data sequence measured at the monitoring nodes and used the predicted value as system feedback to achieve effective control of DO. According to the results, fuzzy PID control algorithm combined with gray prediction outperformed the other two schemes in terms of faster response and smaller overshoots in controlling the dissolved oxygen concentration in RAS.

Regarding oxygen control, in addition to the work introduced earlier by Jie et al., (2019), Zhou et al., (2021, 2022) also considered this water quality parameter in RAS. In the first phase of the study performed by Zhou et al., (2021), empirical transfer functions between aeration flow rate and oxygen content of the water were obtained through open-loop experiments to provide a theoretical basis to analyze the DO control system. Then, this study proposed a differential evolution (DE) algorithm-optimised radial basis function (RBF) neural network proportional integral derivative (PID) controller (DE-RBF-PID). The DE-RBF-PID control scheme uses first the DE algorithm to find the optimal initial parameters of PID. Then the RBF neural network is used to adjust the PID parameters online. Based on the results, the DE-RBF-PID control scheme was able to adjust the PID parameters online and thus eliminate overshoots and improve the controller adaptability compared to the conventional PID and RBF-PID controllers in DO control. In contrast to the experimental model obtained by Zhou et al., (2021), Zhou et al., (2022) proposed a mechanistic model for the oxygen concentration in RAS. Given the established model, that study proposed a fuzzy rule-optimized single neuron adaptive PID controller (FL-SN-PID) for precise control of DO. In the simulation experiment, the DO tracking

performance of the proposed controller was compared with the traditional PID and the single neuron adaptive PID controller (SN-PID). The results of this study demonstrated that FL-SN-PID performed the best to control the DO over the two other controllers in terms of smaller integral of absolute error (IAE) and the integral of squared error (ISE).

In addition to DO and temperature control, denitrification control have also been reported in the literature (Almeida et al., 2020; Lee et al., 2000). Denitrification is also crucial in RAS to maintain nitrate concentrations in accordance with effluent regulations and fish requirements. Lee et al., (2000) used a fuzzy logic-based control system to optimize denitrification rates and eliminate discharge of toxic by-products (i.e., NO_2, NO, N_2O, or H_2S). This was done through monitoring oxidation–reduction potential (ORP) and addition of methanol and water flow rate in the denitrification unit. This fuzzy logic-based control system was capable of maintaining low nitrate concentration while avoiding an increase in NO_2 or H_2S. Almeida et al., (2020) applied a PID control, a linearizing, and a cascade control strategy (combining PI and linearizing controllers where PI controller is used in the outer loop) to control the nitrate level in the denitrification reactor in RAS by addition of acetic acid. Through the addition of an anti-windup action (to avoid detrimental effects due to input saturation), both PID and linearizing controllers could maintain stability. However, in contrast to the linearizing controller, the addition of measurement noise caused some robustness issues in the PID performance. Moreover, the cascade control strategy may also improve the control robustness to model uncertainties, compromising the tracking performance.

From the control studies discussed above, most of the recent contributions on the closed-loop operation of RAS are focused on fuzzy logic based or decentralized controllers such as PI or PID.

Despite several advantages of fuzzy control such as independency of the model and the ability to handle uncertain and nonlinear models, manual tuning of these controllers is time consuming in large-scale applications (Albertos et al., 2000). Furthermore, RAS is a highly interactive system (for example, ammonia concentration is affected not only by the water exchange in the system, but also by aeration rate which influences ammonia removal through nitrification process). This nonlinear, interactive behavior of RAS is caused by the integration of multiple units through the water stream recirculating in RAS (i.e., fish tanks, mechanical filter, biological reactors) as well as the biological reactions taking place in the system. Moreover, none of the proposed control schemes are capable of explicitly taking water quality constraints into account, which is essential to guarantee fish well-being. Thus, to take this behavior into account, application of advanced model-based MIMO (multiple-input, multiple output) controllers would be necessary. Nonlinear model predictive control (NMPC) is a receding horizon control in which a sequence of control actions is obtained by solving an optimization problem at each sampling interval (Mayne et al., 2000). One of the advantages of NMPC over conventional controllers is the ability to explicitly handle constraints, which would become important in providing the optimal rearing environment for fish. Chahid et al., (2021) proposed four MPC control strategies with following purposes: (1) fish growth trajectories tracking, (2) feed and energy consumption reduction, (3) Feed Conversion Ratio (FCR) reduction, and (4) economic profit maximization. The different MPC strategies proposed in this work give the farmer more flexibility to choose the most suitable method as a baseline control strategy for their own needs depending on the type of fish, selling price, culture duration, feed cost, etc. Note that in all of the scenarios considered in that study, a bioenergetic fish growth model

capable of capturing the dominant growth factors (feed ration, oxygen and ammonia concentration as well as temperature) was used to predict fish growth. Among these growth factors, feeding rate, temperature, and dissolved oxygen are used as the manipulated variables for controlling the system, whereas unionized ammonia is a constant known a priori. However, the performance of the proposed MPC strategies should also be evaluated under the case where fish growth model is integrated with a RAS model to represent the actual operation.

To control the system and make efficient decisions at critical times to avoid major losses in the system (e.g., failure of the oxygen supplier unit), online monitoring of the water quality parameters is essential. However, the accuracy and cost of measurement devices in large-scale industrial operations preclude full accessibility to the system's states (Fowler et al., 1994; Valipour et al., 2021). An alternative approach is to use dynamic model-based state estimation techniques to estimate the unmeasurable states. These techniques use the measured values of the system as well as a mathematical model relating the measured/unmeasured variables to estimate the unmeasurable states (Alexander et al., 2020). There are several well-known estimation schemes available in the literature such as Kalman filtering (KF), extended Kalman filtering (EKF), unscented Kalman filtering (UKF), ensemble Kalman filtering (EnKF), particle filtering (PF) and moving horizon estimation (MHE) (Alexander et al., 2020). However, to the author's knowledge, no study has considered application of state estimation methods in RAS; resulting in another gap in the literature.

2.4 Summary

This chapter presented a review of the relevant studies in modeling and control of RAS. In the first section of this chapter, the conceptual framework and background for RAS as well as the main units involved in the operation of these systems were introduced. Section 2.2 presented the current state-of-the-art in modeling of RAS, which is important for analysis, design, and operation of RAS as well as developing control methodologies to control the system. Based on this section, integration of a fish growth model with a RAS model is still missing in the literature. Having access to such model would enable to study the effects of water quality parameters and management strategies on fish growth. Moreover, studies on the closed-loop operation of RAS were also reviewed in this chapter. Most of these control studies for RAS have focused on implementation of fuzzy logic and decentralized controllers. Despite the ability of these control strategies to keep the water quality parameters on target, the application of model-based control schemes is essential to handle the nonlinear, interactive behavior of RAS. However, to overcome the limitations in the available measurements of the system (which is necessary for an adequate performance of the control schemes), the addition of a state estimator layer is of great importance. Application of such estimator on RAS has not been reported in literature.

The work of this chapter has been accepted for publication in the journal of Aquacultural Engineering with minor modifications.

Chapter 3

Dynamic modeling of RAS

A RAS model can be constructed by considering the major units involved in this system (fish rearing tanks, filtration unit, biological reactors, and a system for gas exchange) and integrating them through material streams. Fish welfare is of great importance in aquaculture, thus models presenting fish growth and mortality are incorporated within the RAS model to predict fish performance in RAS as well. In this regard, Section 3.1 explains the dynamic models required to develop the integrated RAS system. This section is then followed by model implementation and validation using experimental data available in the literature to assess the fidelity of the proposed model. Section 3.3 investigates four common scenarios in the operation of RAS together with the detailed discussions of each scenario. Concluding remarks of this chapter are explained in the end.

3.1 RAS model

The major units involved in RAS are comprised of fish rearing tanks, a drum filter, MBBR, and a system for gas exchange (See Fig 2.1). The RAS model in this study is then constructed by representing the four units shown in Fig 2.1 and integrating them through material streams. Note that to predict fish growth, a bioenergetic relation proposed by Ursin, (1967) which is based on anabolism and catabolism processes is used as well. According to this model, growth

can be affected by feeding ration and water quality parameters (e.g. temperature, oxygen concentration). A mortality relationship proposed by Lorenzen, (1996) is also used to express mortality as a function of fish body weight with higher mortalities for smaller fish (Section 3.1.4). To model the MBBR used in this work, the zero-dimensional biofilm model (0DBFM) proposed by Plattes et al., (2008) is used. However, the nitrification process considered in the 0DBFM is adjusted based on the modifications proposed by Ostace et al., (2011) (Section 3.1.2). In general, the RAS model presented in this work considers the following assumptions:

1. The fish tanks are modeled as completely mixed reactors (Wik et al., 2009) where the proposed dynamic mass balances of waste components can predict the influent load to the treatment section.
2. It is assumed that the growth rate is the same for all fish in the tanks.
3. The mechanical filtration stage is assumed to operate at steady state with a constant removal efficiency.

Note that while the proposed model in this study is developed with the focus on salmonids; all the constants and values reported were collected for rainbow trout. As such, this model can be adjusted for any salmonid by altering the tolerances for waste products and optimal growth conditions to the species of interest.

3.1.1 Fish tanks

Estimation of the waste produced in the fish tanks is of critical importance in aquaculture and can influence the design and performance of the treatment section. Feed has been reported to

be the major source of waste in aquaculture (Dauda et al., 2019). This can contribute to the total waste in the water either directly through feed loss or indirectly through undigested or unabsorbed materials (faecal egestion) and metabolic products (branchial and urinary excretion) (Bureau and Hua, 2010). Therefore, the mass balance for a waste component i in a well-mixed fish tank is expressed as follows:

$$V_{tank}\frac{dZ_i}{dt} = Q_{tank}(Z_{i,in} - Z_i) + W_i + L_i \quad (3.1)$$

where Z_i denotes either soluble concentration S_i or particulate concentration X_i, $Z_{i,in}$ is the concentration of waste component i in the tank influent, V_{tank} is the fish tank volume, Q_{tank} is the flowrate, W_i is the production (excretion) rate of waste component i (Wik et al., 2009). L_i represents the amount of waste component i lost to the water through feed loss and can be calculated as follows:

$$L_i = \varepsilon_{loss}\delta_i F(t) \quad (3.2)$$

where $F(t)$ is the feeding rate, ε_{loss} is the feed loss fraction, and δ_i is a constant representing the fraction of component i in the feed. To estimate waste production rate of component i (W_i), the gastrointestinal tract of the fish has been modeled as a perfectly mixed tank (Pedersen, 2018; Wik et al., 2009) i.e.,

$$\tau\frac{dW_i}{dt} = (1 - \varepsilon_{loss})\gamma_i F(t) - W_i \quad (3.3)$$

where τ is the residence time of feed in the stomach and intestine of the fish. This residence time is typically a function of the size of fish (Wik et al., 2009) though it can be assumed

constant when the body weight does not change significantly over a specific period of time. γ_i determines the proportion of the feed that is converted to waste compound i.

Dissolved and particulate organic matter (COD), nitrogen (N), and phosphorus (P) are the main constituents of wastewater in aquaculture (Piedrahita, 2003). Phosphorus removal was not considered in this study due to its low toxicity to fish (Dauda et al., 2019). To simplify the integration of the fish tank material balances with the wastewater treatment units, total nitrogen and organic matter are fractionated into the variables typically used in wastewater treatment models. Accordingly, Z_i in Eq. (3.1) refers to the following variables: soluble inert organic matter (S_I), readily biodegradable substrate (S_S), particulate inert organic matter (X_I), slowly biodegradable substrate (X_S), heterotrophic biomass (X_{BH}), ammonia oxidizing bacteria (X_{AOB}), nitrite oxidizing bacteria (X_{NOB}), particulate products arising from biomass decay (X_P), nitrite nitrogen (S_{NO2}), nitrate nitrogen (S_{NO3}), total ammonia nitrogen (S_{NH}), soluble biodegradable organic nitrogen (S_{ND}), particulate biodegradable organic nitrogen (X_{ND}) and alkalinity (S_{Alk}).

Due to the lack of widely accepted methods for this conversion; particularly for carbonaceous components (Drewnowski et al., 2019), the fractionation method used in this work is only an approximation of the actual values. The readily biodegradable organic matter (S_S) was approximated by the five-day biochemical oxygen demand (BOD_5, Dalsgaard and Pedersen, 2011) and inert soluble matter (S_I) was calculated by subtracting S_S from the total dissolved waste fraction measured by Dalsgaard and Pedersen, (2011). The slowly biodegradable fraction (X_S) was estimated based on the ratio of $BOD_{20}/\ COD$ (Chen et al., 1993) where BOD_{20} is twenty-day biochemical oxygen demand, and COD is chemical oxygen demand. Particulate

inert organic matter (X_I) was determined as the difference between solid COD and X_S. Fractionation of total nitrogen into total ammonia nitrogen (S_{NH}), soluble biodegradable organic nitrogen (S_{ND}), and particulate biodegradable organic nitrogen (X_{ND}) was implemented as reported in the literature (Dalsgaard and Pedersen, 2011).

Table 3.1 summarized the relationships obtained under the assumptions described above and the experimental study conducted by Dalsgaard and Pedersen, (2011). Note that only the variables typically found in the waste produced by the fish are listed in this table. The values of γ_i are estimated based on the solid and suspended/dissolved content of the waste quantified by Dalsgaard and Pedersen, (2011). Similarly, the values of δ_i were obtained from the analysis of a commercial diet for rainbow trout (EFICO Enviro 3 mm, BioMar, Denmark). Composition of this diet along with the apparent digestibility coefficients (ADC) that were used to calculate the digestible fraction of the proximate nutrients in the feed are shown in Table 3.2. $\omega_{protein}$, ω_{lipid} and ω_{NFE} represent the fraction of protein, lipid, and nitrogen free extract in the food, whereas $ADC_{protein}$, ADC_{lipid}, and ADC_{NFE} show the apparent digestibility coefficients of these components respectively.

Table 3.1

Fractionation of feed and waste into typical wastewater treatment model variables.

Variable	γ_i	δ_i
Total ammonia nitrogen	0.337 $N_{ingested}$	-
Soluble organic nitrogen	0.139 $N_{ingested}$	0.29N_{feed}
Particulate organic nitrogen	0.068 $N_{ingested}$	0.71N_{feed}
Readily biodegradable substrate	0.204 $COD_{solid,actual}$	0.145 $COD_{feed,actual}$
Slowly biodegradable substrate	0.61 $COD_{solid,actual}$	0.435 $COD_{feed,actual}$
Inert soluble organic material	0.204 $COD_{solid,actual}$	0.145 $COD_{feed,actual}$
Inert particulate organic material	0.39 $COD_{solid,actual}$	0.275 $COD_{feed,actual}$

$COD_{solid,actual}$= 0.9$COD_{solid,calculated}$

$COD_{solid,calculated}$=$\omega_{protein}(1 - ADC_{protein})1.77 + \omega_{lipid}(1 - ADC_{lipid})2.88 + \omega_{NFE}(1 - ADC_{NFE})1.16$ *

$COD_{feed,actual}$= 0.74 $COD_{feed,calculated}$

$COD_{feed,calculated}$= $1.77\omega_{protein} + 2.88\omega_{lipid} + 1.16\omega_{NFE}$

$N_{ingested}$= N_{feed}= $\omega_{protein}/6.25$

* The values for apparent digestibility coefficients (ADC) along with food compositions (ω) used in this table can be found in Table 3.2.

Table 3.2

Composition of proximate nutrients (EFICO Enviro 3 mm, BioMar, Denmark) and their apparent digestibility coefficients of a commercial diet for rainbow trout.

Component	$\boldsymbol{\omega}$ (%)	$\boldsymbol{ADC}$ (%)
Protein	45	94
Lipid	24	91
N-free extracts (NFE)	15.4	66

Due to lower availability of oxygen in water than in air, aquatic animals are exposed to greater oxygen limitations than terrestrial species (Kramer, 1987). Inadequate oxygen concentration impairs feed intake and fish growth (Magnoni et al., 2018); hence, maintaining the oxygen concentration within an acceptable range is crucial for fish welfare. The following mass balance can be used to estimate oxygen concentration in the fish tanks ($S_{O,FT}$) at any time t:

$$V_{tank}\frac{dS_{O,FT}}{dt} = Q_{tank}(S_{O,in} - S_{O,FT}) \; - \; r_{O2} + m_{O2,FT} \tag{3.4}$$

where $S_{O,in}$ is the oxygen concentration in the inlet flow to the fish tanks; r_{O2} represents the overall oxygen consumption by biomass in the fish tank and is calculated by the relation proposed Liao, (1971):

$$r_{O2} = M(t)C_1T^{C_2}W^{C_3} \tag{3.5}$$

where $M(t)$ is the fish tank biomass (kg), T is temperature, and W is the average fish body mass. The constants C_1, C_2, and C_3 for different species and different temperatures can be found in Liao, (1971). $m_{O2,FT}$ is the oxygen externally added to the fish tanks. The source of this additional oxygen can be aeration, high pressure oxygen gas, liquid oxygen, or on-site oxygen generations such as pressure swing adsorption (PSA) and vacuum swing adsorption (Timmons et al., 2002). For example, in the case of aeration (Wik et al., 2009):

$$m_{O2,FT} = V_{tank}K_{L,O2}(S_{O2,sat} - S_{O,FT}) \tag{3.6}$$

where $K_{L,O2}$ is the mass transfer coefficient and $S_{O2,sat}$ is the oxygen saturation concentration in the water.

The carbon dioxide produced as a result of respiration of the fish and microorganisms can also affect fish physiological functions (Ishimatsu et al., 2005; Khan et al., 2018). Carbon dioxide concentration in the water can be estimated using a similar approach as that used for oxygen, i.e.,

$$V_{tank}\frac{dS_{CO2}}{dt} = Q_{tank}(S_{CO2,in} - S_{CO2}) \; + \; r_{CO2} - m_{removed} \tag{3.7}$$

where r_{CO2} (carbon dioxide production rate) is proportional to the oxygen consumption rate (i.e., $r_{CO2} = \frac{44}{32} r_{O2}$). $m_{removed}$ is the removal rate of carbon dioxide; in the case of aeration, this term can be determined as follows:

$$m_{removed} = VK_{L,CO2}(S_{CO2} - S_{CO2,sat}) \quad (3.8)$$

where $K_{L,CO2}$ is the mass transfer coefficient and $S_{CO2,sat}$ is the carbon dioxide saturation concentration of water.

3.1.2 Biological reactors

Multi-dimensional biofilm models (e.g. 1D, 2D, 3D) have found limited applications within the engineering community due to their complexity. They focus more on the micro-environment and structure of the biofilm and require longer computational times (Plattes et al., 2008, 2006). In this study, a zero-dimensional biofilm model (0DBFM) proposed and validated by Plattes, (2008) is used for modeling the MBBRs since it focuses more on the macro-kinetic behavior of the biofilm system which is of primary importance in this study as the time scale for fish growth is much greater than the micro-kinetic interactions within the biofilm. Diffusional mass transport across the biofilm is not modeled explicitly in this model; instead, diffusional mass transfer limitations are modelled implicitly using adapted half-saturation coefficients in the Monod expressions (Plattes et al., 2006).

The 0DBFM model describes the biochemical conversions in the bulk and biofilm using the widely applied activated sludge model No. 1, ASM1 (M. Henze et al., 1987; Plattes, 2018). In addition to these reactions, expressions describing the attachment of particulates to the biofilm and detachment of particulates into the bulk are added to make it suitable for biofilm

applications. Full details of this model can be found in Plattes et al., (2008), but the key equations regarding the mass balances for dissolved compounds (S_i), suspended particulate components (X_i^S) and biofilm particulates (X_i^B) are as follows:

$$\frac{dS_i}{dt} = (Q_{BR}/\ V_{BR})(S_{i,in}\ - S_i) + r_{0D\ BFM_i} \tag{3.9}$$

$$\frac{dX_i^S}{dt} = (Q_{BR}/\ V_{BR})\left(X_{i,in}^S\ - X_i^S\right) + r_{0D\ BFM}{}_i^S \tag{3.10}$$

$$\frac{dX_i^B}{dt} = r_{0D\ BFM}{}_i^B \tag{3.11}$$

where $r_{0D\ BFM_i}$ is the rate of change of component i, Q_{BR} is flow rate, V_{BR} is the volume of the bioreactor. $S_{i,in}$ and $X_{i,in}^S$ represent concentration of dissolved and suspended particulate components in the influent to the reactor, respectively. Since there are no terms for influent nor effluent to the biofilm, concentration of biofilm particulates only changes with $r_{0D\ BFM}$ (Plattes et al., 2006).

As mentioned in Chapter 2, nitrification is the most important process taking place in MBBRs. This process consists of two steps; in the first step, ammonia is converted into nitrite by ammonia oxidizing bacteria (AOB), whereas in the second step, the produced nitrite is oxidized by nitrite oxidizing bacteria (NOB) to nitrate (Ostace et al., 2011; Pedersen, 2018). Despite nitrification being considered a two-step process, the 0DBFM model considers nitrification as a single-step process. To take this two-step behavior into account, kinetic terms have been adjusted according to the modifications represented by Ostace et al., (2011). Details regarding the reaction terms, kinetic parameters, and stoichiometric coefficients can be found in the supplementary material section of this study.

3.1.3 Fish growth

To assess the performance of RAS under different environmental conditions, there is a need to integrate environmental aspects of the operation with fish growth. Therefore, a bioenergetic model composed of fish anabolism and catabolism processes proposed by Ursin, (1967) is used in this study:

$$\frac{dW}{dt} = \quad bR \quad - \quad abR \quad - \quad KW^n \tag{3.12}$$

According to this model, fish weight increases only when anabolic processes (first term on the right-hand side) are greater than the sum of the catabolic processes of feeding and fasting (second and third term on the right, respectively). In this model, a is the fraction of the food assimilated, b is the efficiency of food assimilation, R is the daily feed intake for one fish, K is catabolism coefficient, and W is the fish body weight. The daily feed intake given to the fish (daily ration) is proportional to fish body weight (FAO,2020) and can be affected by food availability (f) and environmental conditions (E) (M. Varga et al., 2020), i.e.,

$$R = EfhW^m \tag{3.13}$$

where h is the coefficient of food consumption. Food availability (f) is defined as the ratio of the daily ration to the maximum daily ration; with values ranging between zero and one. The effects of dissolved oxygen, unionized ammonia, and temperature on the daily ration can be described as the product of the following piecewise functions:

$$E = \kappa\sigma\upsilon \tag{3.14}$$

$$\kappa = \begin{cases} exp\left\{-4.6\left[\frac{T_{opt}-T}{T_{opt}-T_{min}}\right]^4\right\} & T < T_{opt} \\ exp\left\{-4.6\left[\frac{T-T_{opt}}{T_{max}-T_{opt}}\right]^4\right\} & T \geq T_{opt} \end{cases} \quad (3.15)$$

$$\sigma = \begin{cases} 1 & DO > DO_{crit} \\ \frac{DO - DO_{min}}{DO_{crit} - DO_{min}} & DO_{min} \leq DO \leq DO_{crit} \\ 0 & DO < DO_{min} \end{cases} \quad (3.16)$$

$$\upsilon = \begin{cases} 1 & A < A_{crit} \\ \frac{A_{max}-A}{A_{max} - A_{crit}} & A_{crit} \leq A \leq A_{max} \\ 0 & A > A_{max} \end{cases} \quad (3.17)$$

where κ, σ and υ represent the effect of temperature, dissolved oxygen, and unionized ammonia, respectively, and T, DO and A represent temperature, dissolved oxygen, and unionized ammonia concentrations in the fish tank, respectively. Under optimal conditions, the outputs of these piecewise functions would be one and decrease gradually as conditions deviate from optimum and finally reach zero when environmental parameters cross their critical values (Dampin et al., 2012). The concentration of unionized ammonia is required for Eq. (3.17) and can be calculated as follows (Fivelstad et al., 1995):

$$A = \frac{1}{1+antilog(\left(pK_a{}^0+S_k+0.0324(24.85-T)\right)-pH)}\ TAN \quad (3.18)$$

where TAN is the total ammonia nitrogen (sum of ionized and unionized ammonia). $pK_a{}^0$ is the ionization constant for ammonium ion at 25°C and zero ionic strength; T is the temperature in degrees Celsius, and s_k is the salinity of water.

The catabolism coefficient (K) in Eq. (3.12) is temperature dependent and can be described as follows (Dampin et al., 2012; Ursin, 1967) :

$$K = K_{min} \exp\ [J(T - T_{min})] \quad (3.19)$$

where K_{min} is the coefficient of fasting catabolism at T_{min}, J is a constant, and T_{min} is the minimum temperature at which a fish can survive. Efficiency of food assimilation (b) which is a function of fish body weight (W) (Dampin et al., 2012) can be estimated as follows:

$$b = b_1 \log\,(b_2 W) \quad (3.20)$$

This relationship was fitted using experimental data from Kolarevic et al., note that b_1 is -0.208 and b_2 is 0.006.

3.1.4 Mortality and number of fish

In all RAS operations, the number of fish in the tanks decreases as a function of time due to fish mortality. The Beverton–Holt recruitment model describes the number of fish (NF) in the tanks at any time t:

$$\frac{dNF}{dt} = -M_{ins} NF \rightarrow \mathrm{NF} = N_0\, e^{-M_{ins} t} \quad (3.21)$$

where M_{ins} is the instantaneous mortality rate and N_0 is the initial number of fish (van Poorten et al., 2018). In culture systems (e.g., tanks, ponds, or cages) compared to natural systems (e.g., rivers, oceans), non-predation mortality is more important than predation mortality. Non-predation mortality is thought to be related to the incomplete immune systems of fish, increased susceptibility to abiotic conditions, and reduced energy storage (Lorenzen, 1996; Ursin, 1967). Natural mortality rates of fish are closely related to body weight (Lorenzen, 1996; Ursin, 1967), i.e.,

$$M_{ins} = M_u\, W^{-c} \quad (3.22)$$

where M_u is natural mortality rate at unit weight, and c is the allometric scaling factor.

3.2 Model implementation and validation

The model was validated using experimental data from an 8.5 m^3 RAS stocked with rainbow trout (Fernandes et al., 2017). The system is composed of a 5.5 m^3 fish tank, a trickling filter, four biofilters (two fixed bed biofilter (FBB) and two MBBRs), and a 40 μm drum filter (Table 3.3). The experiment consisted of an initial 8-week acclimatization and maturation period followed by a 6-week testing period. This testing period was divided into four phases; two phases where all filters were in operation and two phases where only one type of biofilter was in operation (FBB or MBBR). For the purpose of validation, it is assumed that the MBBRs remained in operation at all times. Both MBBRs were filled with RK BioElements with a density of 1.0 g/cm^3 and assumed to be identical. A detailed explanation of the experimental setup can be found in Fernandes et al. (2017).

Table 3.3

Experimental data from Fernandes et al. (2017) MBBR trials.

Property	Value
Initial biomass	*130 kg*
Fish initial body weight	*45 g*
Fish tank volume	5.5 m^3
Biofilter volume	0.4 m^3
Water flow to each biofilter	7.2 m^3/hr

The following assumptions were made in the model validation:

1. It is assumed that nitrification only occurs in the MBBRs and that the contribution of the trickling filter to nitrification is negligible; thus, the only function of the trickling filter is for aeration and carbon dioxide degassing (Pedersen et al., 2012).

2. The drum filter is assumed to operate at steady state with 48% removal efficiency (Timmons et al., 2002).

3. It is assumed that oxygen concentration, alkalinity, temperature, and pH were kept constant at 8 mg/L, 118 $mg\ CaCO_3/L$, 19.5℃, and 7, respectively.

4. Biomass was removed during the experiment to keep the stocking density within the range of $35 \text{ and } 50\ kg/m^3$. Since the exact value was not available, it is assumed that the final stocking density is $35\ kg/m^3$.

5. The experimental feeding rate was reported to gradually increased until a rate of $2\ kg/day$ was reached. As the interim values were not explicitly stated, the feeding rate is calculated based on the fish bodyweight using Eq. (13) and the difference is assumed to be negligible. Despite the changing ration, the ratio of feed loading to make-up water flow rate was held constant at 1 kg/m^3 . Additionally, it is assumed that feed was allocated between 9:00 and 15:00 daily.

6. It is assumed that feed spillage is 3% of the feeding rate.

The RAS model consists of 64 states (i.e., 64 ordinary differential equations). The model was implemented in Python 3.6 and Lsoda from the Scipy package was selected as the solver for the set of differential equations involved in the model. Lsoda can automatically switch between stiff

(backward differentiation formula) and non-stiff (Adams) methods depending on the behavior of the problem. To validate the model, the RAS system was allowed to evolve dynamically for 98 *day*s (i.e. the experimental period) before it was compared to the data reported by Fernandes et al., (2017). Note that in this time the system had reached a steady state of operation. The values of the model parameters and the initial conditions used for validation can be found in the nomenclature.

Table 3.4

Comparison of steady-state values of the RAS model and the experimental data from Fernandes et al. (2017).

Variable	RAS model	Experimental Data
$TAN\ (mg\ N/L)$	0.49	0.26 ± 0.03
$NO_2 - N\ (mg\ N/L)$	0.32	0.22± 0.02
$NO_3 - N\ (mg\ N/L)$	37.58	44.3 ± 1.2
$COD_{TOT}\ \ (mg\ O_2/L)$	44.43	26.5 ± 2.5
$BOD_{5TOT}\ (mg\ O_2/L)$	1.48	5.5 ± 0.4
$BOD_{5FILT}\ (mg\ O_2/L)$	0.97	1.8 ± 0.1
$BOD_{5PART}\ (mg\ O_2/L)$	0.51	3.7 ± 0.4
Mortality	0.2%	0.1 %

As shown in Table 3.4, the results from model prediction overall are consistent with the experimental values, while some differences are observed. Two of the most important parameters; the TAN and nitrite concentration; were predicted to be higher than the experimental values whereas the nitrate concentration is lower than the reported value. As mentioned before, nitrate is the end product of nitrification. Higher predicted TAN and lower nitrate concentrations indicate that the rate of nitrification is lower in the model under the assumptions made. These differences can partly be explained by the fact that nitrification can

occur in the trickling filter as well as the MBBRs, which was assumed to be negligible in this model. Moreover, Fernandes et al., (2017) reported higher TAN and nitrite concentrations when only MBBRs were in operation compared to when fixed bed biofilters were in operation. This model assumes that only MBBRs are in operation for the entire experimental period which may explain the higher predicted ammonia and nitrite concentrations.

It is also highly possible that the method used for fractionation of the carbonaceous parts of the waste into the typical parameters used in wastewater treatment models is flawed as there is no generally agreed upon method for making this conversion. Finally, higher predicted values of total organic matter compared to experimental data may be due to the small differences in feeding rate and the assumptions made related to stocking densities used in the experiment. One significant challenge in developing RAS models is the lack of robust validation data.

To further validation of the model, the concentration of waste components at different feeding rates was analyzed. For further validation of the model, Table 3.5 shows that increasing feeding rate from 4 kg/day to 8 kg/day results in an increase in the concentration of all waste components, which is in agreement with previous reports. That is, the waste concentration in the water can increase by increasing the feeding since food is the main contributor to the waste generation through feed loss or the waste by-products (Dauda et al., 2019).

Table 3.5

Comparison of RAS operational data at steady state at different feeding rates.

	Feeding rate		
Variable	$4kg/day$	$6kg/day$	$8kg/day$
$TAN\ (mg\ N/L)$	0.18	0.24	0.30
$NO_2 - N\ (mg\ N/L)$	0.11	0.15	0.19
$NO_3 - N\ (mg\ N/L)$	36.99	37.00	37.11
$COD_{TOT}\ (mg\ N/L)$	40.3	41.19	42.11

3.3 Model analysis under different scenarios

Fish growth performance is the most significant element influencing economic viability of the system in commercial aquaculture facilities (Baer et al., 2011). Understanding the effects of different conditions on fish growth can provide farmers with the information needed to make rational decisions that would improve fish welfare and enhance RAS economy.

A set of scenarios are considered to assess fish performance under different water quality parameters and different management strategies. The first scenario (A) investigates the impacts of oxygen concentration which directly affects fish growth and metabolism (Magnoni et al., 2018; Remen et al., 2012). Scenario B investigates the effects of temperature. Fish are poikilotherms (Finn and Nielsen, 1971), i.e., their internal body temperature is controlled by the temperature of the environment which in turn results in changes in food intake and thus fish growth (Jonsson et al., 2001). Maintaining water temperature within the optimal growth range is critical for the effective operation of this process.

RAS systems are relatively new technologies that are still under development; studies that increase our understanding of their performance and management is crucial for the

advancements of these systems. Increasing water reuse and decreasing water exchange rate is necessary to transition from flow through systems to highly recirculated RAS. Scenario C investigates the effect of reducing the water exchange rate on nitrate accumulation to assess the case where the addition of a denitrification unit becomes necessary for successful operation of the RAS. Finally, fish feed is one of the largest operating expenses and thus improving the feeding regime is a common management strategy in fish culture and has been assessed in Scenario D.

Specific growth rate (SGR) proposed by Grover and Brett, (1979) is used as a criterion for quantitative comparison of growth under the different scenarios described above, i.e.,

$$SGR = \frac{logW_t - logW_i}{t_p} \tag{3.23}$$

where W_t is the final body weight, W_i is the initial weight, t_p is the assessment duration.

In all the scenarios presented, the values of the model parameters, operating conditions, and initial conditions are the same as those considered in the model validation section. In all cases, the simulation time was set to 98 days, which agrees with the time horizon considered in previous modelling studies and correlates to the 8 weeks of acclimatization followed by 6 weeks of experimentation used by Fernandes et al. (2017).

3.3.1 Scenario A: the effects of oxygen concentration on growth

The sensitivity of fish welfare to dissolved oxygen concentration (DO) is considered first. DO ranging between 5-7 mg/L was considered as rainbow trout have a critical DO of 6.8

mg/L. According to Remen et al., (2016), oxygen concentrations higher than the critical value (DO_{crit}) results in the maximum feed intake and fastest fish growth. For rainbow trout, in the case where DO is maintained at 7 mg/L , the fish are expected to have the highest growth rate with a SGR of 0.64% per day, as shown in Table 3.6 and Fig 3.1.

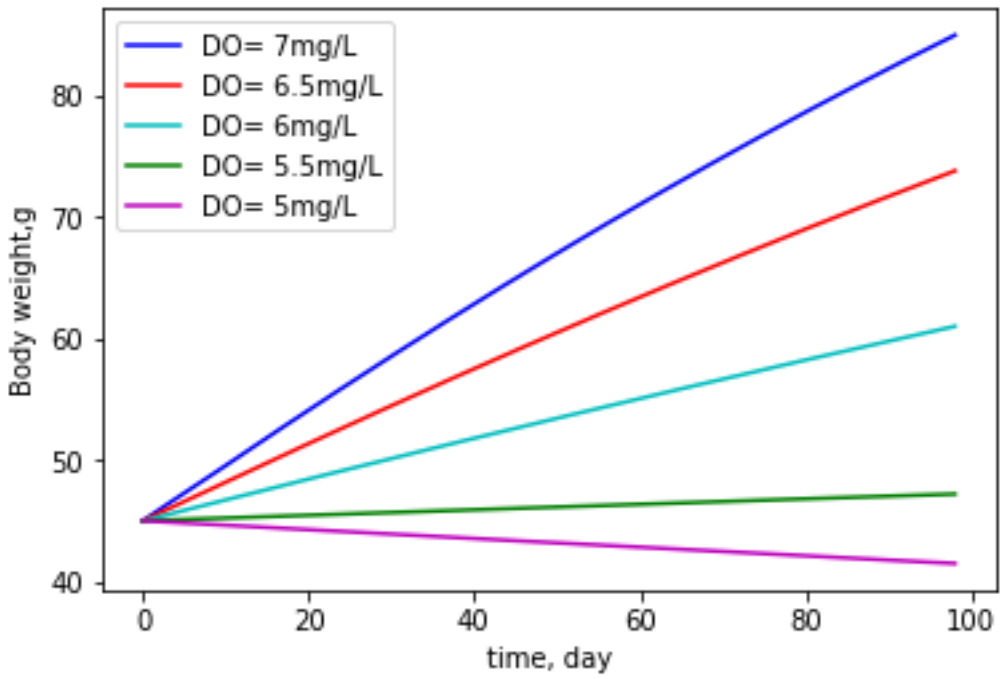

Fig 3.1 Effect of dissolved oxygen concentration on fish growth.

For the lowest case considered (DO = 5 mg/L), fish growth is drastically affected with a SGR of -0.08 % per day. The negative sign indicates that the fish are losing weight. This is expected since a DO of 5 mg/L is lower than the minimum oxygen concentration ($DO_{min} = 5.3\ mg/L$). This is the minimum concentration required for aerobic metabolism and respiratory stress and mortality occur below this level (Noble, 2020; Remen et al., 2016). For values between the $DO_{min} and\ DO_{crit}$, body weight decreases with decreasing oxygen concentration and the calculated SGR drops from 0.5 % per day to 0.04 % per day as the DO approaches DO_{min}, as

shown in Fig 3.1 and Table 3.6. Thus, maintaining oxygen concentration is critical for optimal growth and must be carefully monitored and adjusted using aerators or oxygen generator.

Table 3.6

Specific growth rate of fish under different dissolved oxygen concentrations.

Dissolved oxygen ($mg\ /L$)	**SGR (% per day)**
7	0.64
6.5	0.50
6	0.31
5.5	0.04
5	-0.08

3.3.2 Scenario B: the effects of variation in temperature on growth

Trout can grow within a rather large range of temperatures between 1–25 °C with an optimal near 16°C (Woynarovich, 2011). At overly low or high temperatures, fish health is severely impacted, and feeding will be suspended. This is illustrated in Fig 3.2, where the body weight is highest between 12-16℃, and negatively affected by further deviations of this optimum.

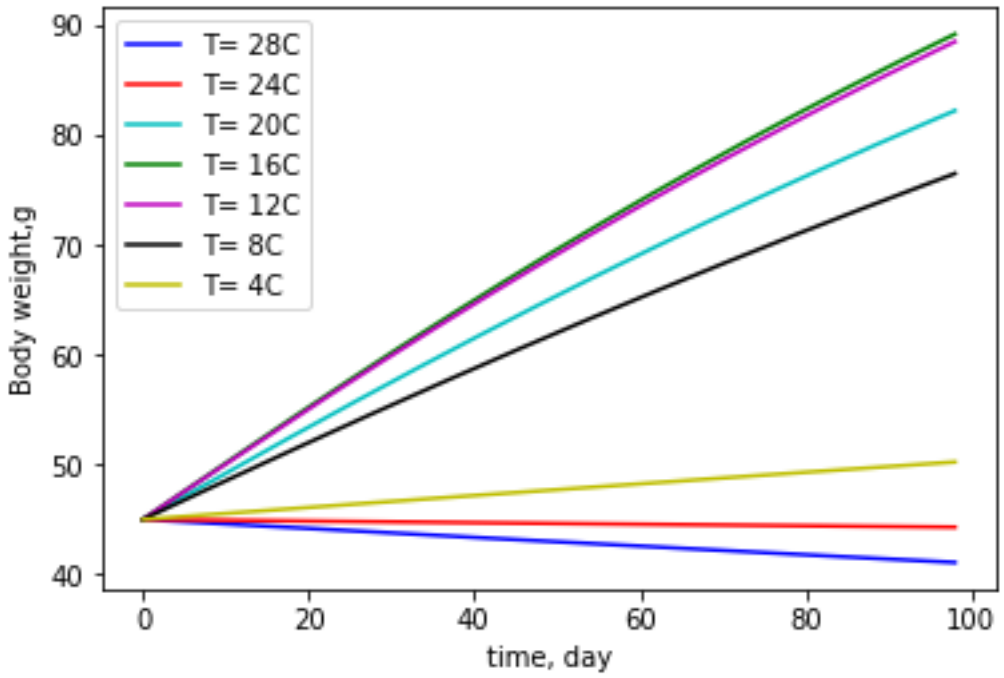

Fig 3.2 Effect of temperature on fish growth.

As shown in Table 3.7, the predicted SGR is the highest at 16℃ (0.7% per day). As temperature deviates from 16℃, SGR decreases until it becomes negative at very elevated temperatures (i.e., above 24℃). At low temperatures, growth proceeds slowly but these temperatures are not damaging to fish welfare. These results agree with previous observations reported in the literature (Woynarovich, (2011)).

Table 3.7

Specific growth rate of fish at different temperatures.

Temperature ℃	**SGR (% per day)**
28	-0.09
24	-0.01
20	0.61
16	0.70
12	0.69
8	0.54
4	0.11

3.3.3 Scenario C: the effects of water exchange rate on growth

Increasing water reuse in RAS is unavoidably accompanied by the accumulation of waste products in the recirculated water in the absence of adequately sized water treatment units. Nitrate; which is an end-product of nitrification process, can accumulate in the absence of a denitrification unit and may reach concentrations that are toxic to the fish.

The ratio of make-up flow rate to feeding rate has been used to express the degree of recirculation. In conventional recirculating systems, this ratio is within $0.1 - 1\ m^3/kg$ feed whereas the next generation of RAS is targeting a much lower exchange rate of less than $0.1\ m^3/kg$ feed in order to reduce water consumption (Martins et al., 2010). In the experimental work conducted by (Fernandes et al., 2017) this ratio was set to the unity. This scenario is concerned with lower ratios of make-up flow rate to feeding rate to investigate the effect of degree of recirculation on nitrate accumulation and indirectly on fish growth.

According to Davidson et al. (2014), rainbow trout begin to exhibit health problems when the ratio of make-up flow rate to feeding rate is below 0.24, which they postulated may be due to the accumulation of nitrate. The recommended upper limit of nitrate concentration for rainbow trout in RAS is 75 $mg\ /L\ NO_3 - N$ (Davidson et al., 2014). As shown in Fig 3.3, for make-up flow rate to feeding rate ratios higher than 0.2 (as suggested by Davidson et al., (2014)), the predicted nitrate concentration is within the safe range for rainbow trout. However, when decreasing this ratio to 0.06, the nitrate concentration can reach to toxic values (e.g., > 600 mg/L). Thus, to safely operate the RAS system under low make-up flow rate to feeding rate ratios, the addition of a denitrification unit would be necessary to avoid nitrate accumulation in

the system. This illustrates the utility of this model which can be used to inform the operational ranges of a particular design, or to inform the design process for next generation RAS.

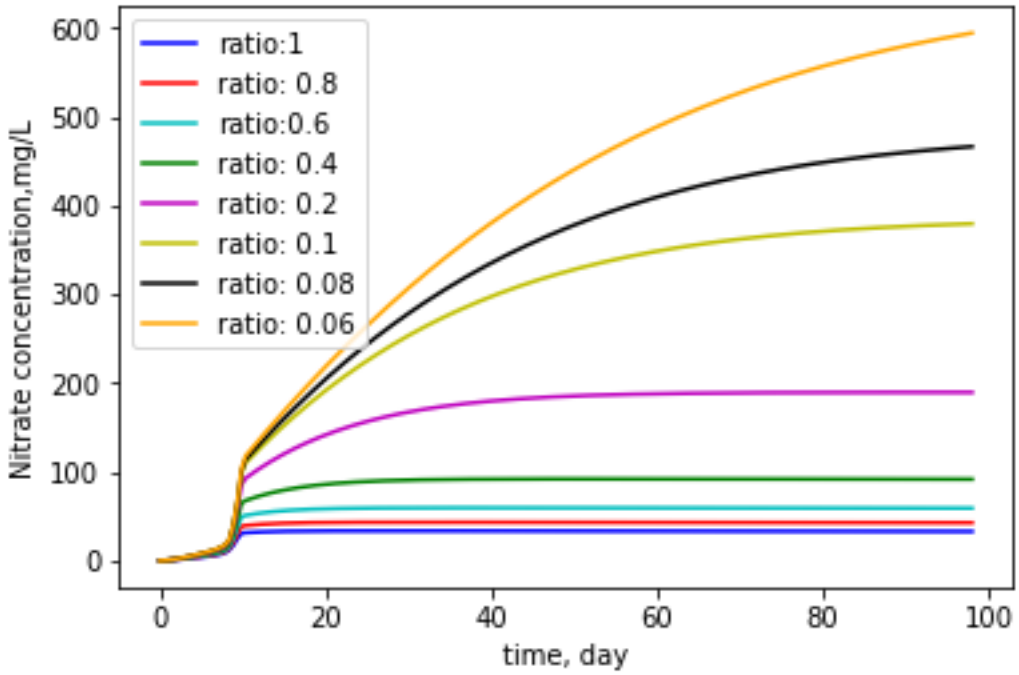

Fig 3.3 Effect of ratio of make-up flow rate to feeding rate on nitrate accumulation.

3.3.4 Scenario D: effect of feeding regime

The cost associated with aquaculture feed represents 40–75% of aquaculture production cost (Ansari et al., 2021); thus, investigating the effects of feeding regimes on fish growth are of interest to the aquaculture industry. In this final scenario, the effect of feeding regime on fish growth was investigated under three different cases. For all of the cases presented, the total daily ration is the same and is estimated from Eq. (3.13); however, the feeding rate is adjusted based on a feeding time span of 6 hours (Case 1), 12 hours (Case 2), or 24 hours (Case 3) and given to the fish continuously during the indicated time span.

As shown in Table 3.8, the differences in SGR among the different feeding regimes is negligible. This indicates that the proposed feeding regimes may not have a significant effect on fish growth. These results agree with a previous study that indicated that feeding frequency does not directly affect growth for a restricted daily ration (Grayton and Beamish, 1977). According to this study, increasing the frequency of feeding in hatcheries can help to reduce food wastage; however, this may not be the case for fish fed to satiation who may feed less later in the day resulting in uneven fed loss. As shown in Fig. 5, increasing feeding duration can also help reduce fluctuations in the waste load entering the treatment section. While MBBRs are robust units that can accommodate fluctuations or shock loads in wastewater, larger fluctuations will require larger unit capacities. Based on these results, Case 1 has the highest fluctuations whereas no fluctuations are observed during Case 3. Thus, continuous feeding (i.e., Case 3) is preferred in terms of waste management and economy in RAS.

Table 3.8

Specific growth rate of fish under different feeding regimes.

Feeding regime	**SGR (% per day)**
6-hour feeding	0.6485
12-hour feeding	0.6486
Continuously	0.6486

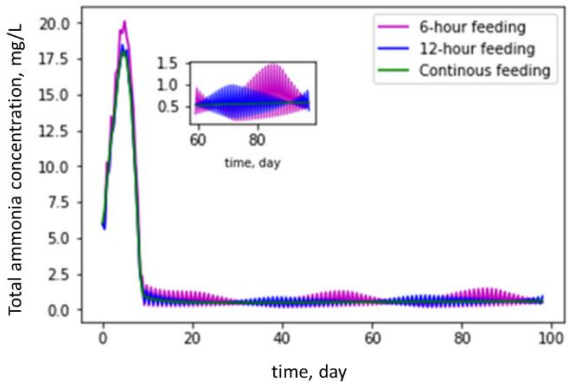

Fig 3.4 Effect of feeding regime on total ammonia concentration in the fish tank.

3.4 Summary

In this study, a dynamic model for RAS was presented and validated using experimental data reported in the literature. The model predictions were consistent with the experimental data and agreed with multiple observations reported in previous studies.

In the present model, fish performance has been integrated with the entire RAS system to provide a tool to gain new insights and hence lead to more informative decisions regarding the operation of RAS while ensuring fish welfare. This was demonstrated by investigating the effects of different water quality parameters on fish growth. Moreover, the impact of feeding regimes on the accumulation of wastes in the system was evaluated. In this regard, continuous feeding was found to result in less fluctuations which is more desirable for the efficiency of wastewater treatment. Furthermore, this model can be used to determine the operational ranges of next generation RAS or inform new RAS designs to increase the sustainability of aquaculture, such as under what conditions a denitrification unit is required.

Chapter 4

Closed-loop operation of RAS using advanced model-based state estimation and control schemes

The quality of the water in the rearing environment has major impacts on feed utilization, fish health, growth, and survival rate (Fowler et al., 1994). Thus, critical water quality parameters such as dissolved oxygen and concentration of waste components should be constantly controlled to ensure fish well-being. Closed-loop operation of RAS with the purpose of keeping the water quality parameters in accordance with the fish needs is investigated in this chapter. To this aim, a nonlinear model predictive controller (NMPC) integrated with moving horizon estimation (MHE) has been implemented in RAS to evaluate the system performance under full and partial access to the system's states in the presence of process uncertainty and measurement noise. As in the previous chapter, several common scenarios in the operation of RAS such as failure of a unit and malfunction of a sensor are considered to further analyze the closed-loop performance of the system. Note that the RAS model introduced in Chapter 3 is the basis for this analysis. Section 4.1 outlines the major modifications and further assumptions made on the RAS model as well as the biological constraints required for fish welfare and considered in the present analysis. Section 4.2 to 4.4 elaborate more on the sensors and instrumentation in RAS along with concepts and formulations of the MHE and NMPC respectively. Section 4.5 presents the different scenarios considered to evaluate closed-loop performance of RAS together with detailed discussions of the results. A summary of this chapter is presented at the end.

Closed-loop operation of RAS

Sufficient supply of oxygen and nutrients in addition to effective waste removal is of primary importance to enable a smooth operation of RAS. Failure in any of the waste removal units or oxygen supply can cause significant losses within a short period of time due to high fish stocking densities and low water exchange in RAS (Fowler et al., 1994). To this regard, continuous monitoring and controlling of RAS are necessary to ensure fish well-being, achieve higher growth rate, and thus enhance profitability of the system (Fowler et al., 1994).

As discussed in Chapter 2, there have been several efforts in the literature to control the quality of the water within the RAS (e.g., temperature and oxygen concentration) through application of fuzzy logic based or decentralized controllers such as PI (proportional–integral controller), or PID (proportional–integral–derivative controller). Despite their success in controlling the quality of water using decentralized SISO (single-input single output) controllers, the application of advanced MIMO controllers (multiple input -multiple output) would be necessary to control multiple water quality parameters simultaneously thereby improving the closed-loop performance of this system. Application of these MIMO controllers in RAS is of great importance due to the strong interaction between the fish rearing tanks and the wastewater treatment section as well as the high water recirculation in the system (Wik et al., 2009). Moreover, the wastewater treatment and the biological reactions that take place for waste removal are complex and highly nonlinear (Han & Qiao, 2014). Accordingly, implementation of an advanced control technique such as NMPC would be crucial to ensure a smooth operation of this process in the presence of external perturbations or changes in the operating conditions of the process. NMPC can also take into account the biological constraints that are critical for fish

welfare such as the maximum allowed concentration of toxic components or minimum dissolved oxygen required for fish growth.

The basic NMPC scheme used to control the system is illustrated in Fig 4.1. In NMPC, at each time interval k, the current control action is obtained by solving a nonlinear dynamic optimization problem (Mayne et al., 2000). This optimization problem is formulated in a way to force the predicted output to reach its setpoint within a finite time horizon (namely prediction horizon) while respecting the constraints (Mayne et al., 2000; Segovia et al., 2019). The solution of this problem yields a sequence of control actions whereas only the first control action is sent to the plant and the rest of the sequence is discarded. This procedure is repeated at each time interval k (Segovia et al., 2019). In the standard NMPC scheme, the current state of the system is used as the initial condition for the states for the next NMPC calculation; thus, full access to the states is key for an adequate performance of the NMPC. However, the cost and the accuracy of the measurement devices in RAS may limit the number of measurable states and hence impact the performance of the NMPC (Fowler et al., 1994; Valipour & Ricardez-Sandoval, 2021). Thus, the addition of an observer that can reconstruct the system's states by estimating the unmeasurable states is of the utmost importance for the efficient operation of a closed-loop system. MHE is the technique of interest in this study due to the ability to handle nonlinearity and high interactions in the RAS as well as the biological constraints inherent for fish health. To estimate the system's states at time interval k, MHE applies an optimization-based framework that uses a process model together with a series of past and current measurements up to current time interval. Note that, only a finite size horizon of the latest measurements is used by MHE for state estimation where this finite horizon (namely moving

horizon) is shifted in time to consider the most recent information (Segovia et al., 2019). The solution of the optimization problem in MHE provides the optimum values for the states at time interval k. At the next time interval $k+1$, as new measurements become available, the moving horizon shifts in time to update the measurements used within MHE calculations and then, the entire process is repeated in an iterative manner to compute the next optimal values of the states (Segovia et al., 2019).

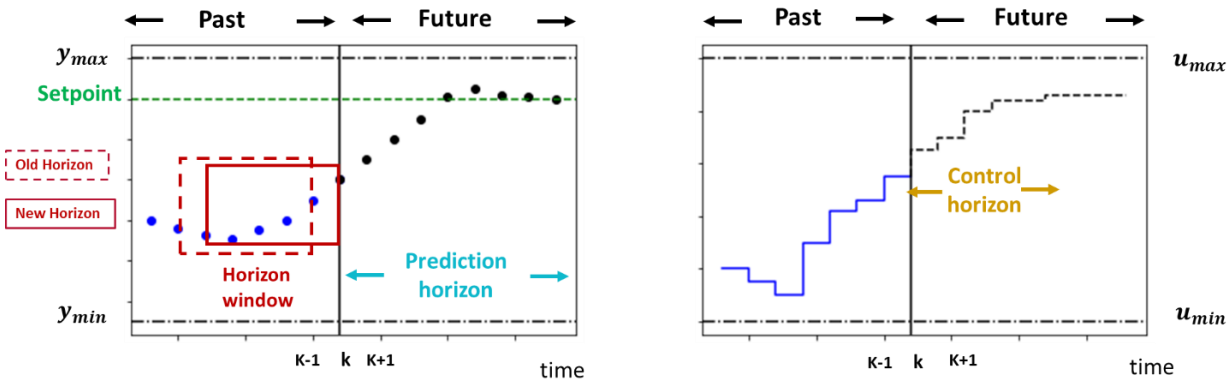

Fig 4.1 A schematic of prediction horizon, control horizon, and moving horizon used in NMPC and MHE formulations respectively (y: controlled variable, u: manipulated variable).

Fig. 4.2 illustrates the closed-loop framework proposed in this work for RAS. The main purpose of this framework is to provide a good rearing environment in terms of sufficient dissolved oxygen and low waste concentrations. In order to achieve this goal and obtain higher fish growth rate; as depicted in Fig 4.2, multiple units need to work together. RAS system (plant) is one of the most important units shown in Fig 4.2. This plant is composed of fish tanks which are the rearing environment for fish as well as the mechanical filter and biological reactors used for waste removal. Note that the states of this plant (i.e., concentration of waste components as well as the oxygen concentration) which may be corrupted with process noise, are important to

control the system and maintain fish welfare. Thus, a few of the plant states can be measured online by the available sensors in the system which may contain measurement noise. The plant's states that cannot be measured are estimated by the MHE embedded in the proposed closed-loop system, as shown in Fig. 4.2. The estimated states together with the process measurements are then used as inputs to the NMPC to compute control actions such that the quality of the water in the fish tanks is always maintained within the range compatible with the fish needs.

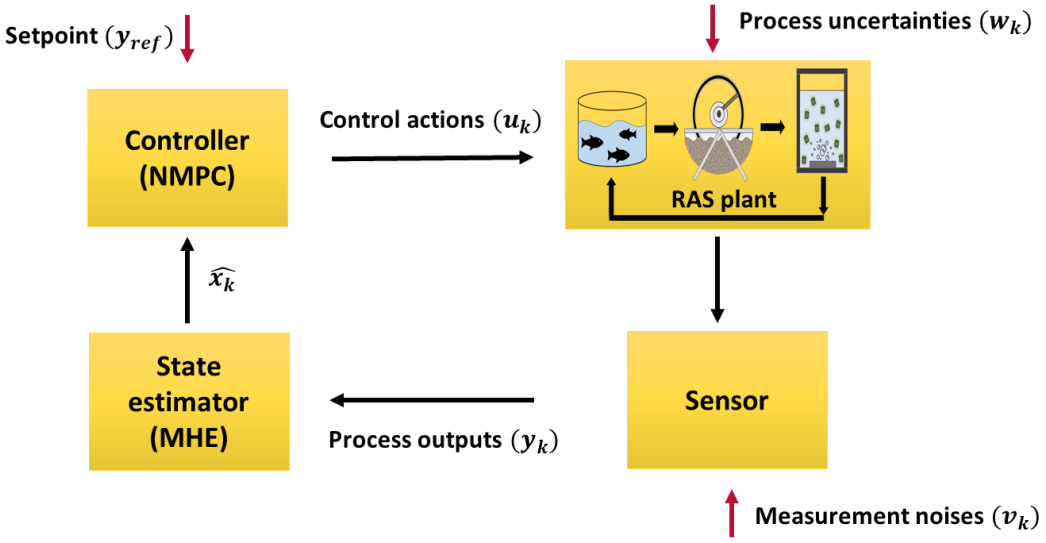

Fig 4.2 Block diagram of closed-loop operation of RAS.

A detailed explanation of the main units shown in Fig. 4.2 is explained next.

4.1 RAS Plant

As discussed in Chapter 3, estimation of the produced waste and the consumed oxygen within the RAS system is important to ensure fish well-being and make informed decisions regarding

the operating conditions, design, and sizing of the major units in RAS. To this aim, a dynamic model was introduced in Chapter 3 to predict the concentration of oxygen and waste components within the RAS. This model presented through Eq. (3.1) to (3.11) represent the basis for the closed-loop implementation presented in this chapter. An assumption made in the RAS model used in this chapter is that fish growth has not been considered; this is because fish growth has slower dynamic compared to the other states in the system (such as concentration of oxygen and waste components). Hence, the present study assumes that changes in the fish size within the period of concern is small and do not have significant influences on the waste production and oxygen consumption in the system.

Note that the water quality parameters in the fish tank should be maintained within the range compatible with fish requirements. That is, the water in the fish tank should meet certain biological constraints, which may vary from one species to another. The most important water quality constraints needed to be satisfied to guarantee fish well-being are discussed next.

- **Oxygen**

Oxygen is key for fish metabolism and growth (Remen et al., 2016). According to Remen et al., (2016), oxygen concentrations higher than a critical value (DO_{crit}) results in the maximum feed intake and fastest fish growth; thus, maintaining oxygen concentration ($S_{O,FT}$) above DO_{crit} is of great importance in RAS (Noble, 2020), i.e.,

$$S_{O,FT} \geq DO_{crit} \tag{4.1}$$

Note that this critical value for oxygen is temperature dependent and should be adjusted according to the operating temperature of the system.

- **Ammonia**

Ammonia concentration is another important water quality parameter. This component is the product of protein catabolism in fish and exists in equilibrium with its much less toxic ionized form: ammonium (NH_4^+). Concentration of total ammonia (S_{NH}) (sum of ionized and unionized ammonia or TAN) should be kept less than an upper limit (UL_{NH}) where this limit is species dependent:

$$S_{NH} \leq UL_{NH3} \tag{4.2}$$

- **Nitrate**

Nitrate concentration is another parameter that needs to be monitored in RAS. Nitrate is the end product of nitrification (a process that converts ammonia to nitrate) and due to low branchial permeability, nitrate has less toxicity for fish (Camargo et al., 2005). However, it is suggested to keep nitrate concentration (S_{NO_3}) in RAS below a recommended value (UL_{NO3}) to avoid changes in the fish's swimming behavior, decreased survival and reduced total biomass (Davidson et al., 2014) , i.e.,

$$S_{NO_3} \leq UL_{NO3} \tag{4.3}$$

4.2 Sensors

To be aware of the prevailing conditions in the rearing environment and act properly under unexpected situations (e.g., failure in the oxygen supply and subsequent drop in oxygen concentration), online monitoring of RAS through the available sensors in the system is needed.

Temperature, dissolved oxygen (DO), pH , salinity, alkalinity, concentration of ammonia, nitrite, nitrate, suspended solids, and biochemical oxygen demand are the primary water quality parameters that should be constantly monitored to control the system and ensure fish welfare (Fowler et al., 1994). However, the high cost of some measurement devices for RAS (e.g., DOprobe) together with the unreliability of the available sensors prevent farmers and stakeholders in this field to monitor and control all of these parameters (Fowler et al., 1994). Recent developments in solid state electronics has improved the reliability and accuracy of these sensors and thus has increased their application in RAS (Fowler et al., 1994).

4.3 Moving Horizon Estimation (MHE)

MHE aims to estimate the unmeasurable states by minimizing the L_2 norm of the process uncertainty and measurement noises over a finite horizon of the last N measurements while satisfying the process constraints (Valipour & Ricardez-Sandoval, 2021). As shown in Fig 4.1, this finite horizon is shifted in time as new measurements are available to the system (Segovia et al., 2019). The general formulation of the MHE is as follows (Segovia et al., 2019) :

$$\min_{\{x_j, w_j\}_{j=k-N}^{k-1}} \quad \sum_{j=k-N}^{k-1} \|w_j\|^2_{\boldsymbol{Q}^{-1}} + \sum_{j=k-N+1}^{k} \|v_j\|^2_{\boldsymbol{R}^{-1}} + \varphi_{k-N} \tag{4.4.A}$$

s.t.

$$x_{j+1} = F(x_j, u_j) + w_j \qquad \forall\, j = k-N, \dots, k-1 \tag{4.4.B}$$

$$y_j = H(x_j, u_j) + v_j \qquad \forall\, j = k-N+1, \dots, k \tag{4.4.C}$$

$$G(x_j, u_j, w_j, y_j) \qquad \forall\, j = k-N, \dots, k \tag{4.4.D}$$

$$x^l \leq x_j \leq x^u \qquad \forall\, j = k - N, \ldots, k \tag{4.4.E}$$

$w \in \mathbb{R}^{n_x}$, $v \in \mathbb{R}^{n_y}$, $x \in \mathbb{R}^{n_x}$, $y \in \mathbb{R}^{n_y}$, $u \in \mathbb{R}^{n_u}$, $\boldsymbol{Q} \in \mathbb{R}^{n_x \times n_x}$, $\mathbf{R} \in \mathbb{R}^{n_y \times n_y}$, $x^l \in \mathbb{R}^{n_x}$, $x^u \in \mathbb{R}^{n_x}$, $F: \mathbb{R}^{n_x \times n_u} \rightarrow \mathbb{R}^{n_x}$, $H: \mathbb{R}^{n_x \times n_u} \rightarrow \mathbb{R}^{n_y}$, $G: \mathbb{R}^{n_x \times n_u \times n_x \times n_y} \rightarrow \mathbb{R}^{n_g}$

As shown in Eq. (4.4.A) to Eq. (4.4.E), k represents the current time interval of the system whereas j is the time interval in the moving horizon. N is the length of the moving horizon; $\boldsymbol{Q}$ and $\boldsymbol{R}$ are the covariance matrices of process uncertainties and measurement noises; w and v are vectors that describe the process uncertainty and measurement noise, respectively. To estimate the system's states, MHE relies on both plant measurements and a plant model which may contain noises (v and w respectively). However, out of these two sets of information, MHE will follow the one with lower covariance ($\boldsymbol{R}$ or $\boldsymbol{Q}$) or lower distribution which further indicates higher reliability of that distribution (Valipour & Ricardez-Sandoval, 2021). x is the vector of states in the RAS consisting of the concentration of oxygen and waste components in the system. u is the set of input variables that can be adjusted online for control. y is a vector representing the available measurements in the system. Note that the vector of available measurements includes the states that are measured directly, e.g., ammonia and oxygen as well as the quantities consisting of multiple states, e.g., chemical, and biological oxygen demand (see Table 4.3). The process model is denoted by F and is described by Eq. (3.1) to Eq. (3.11) whereas H shows the relationship between the measurements and the states (see Table 4.3). Function G represents the inequality constraints while x^l and x^u are the vectors representing the lower and upper bounds on the states. Eq. (4.1) to Eq. (4.3) represent the inequality constraints considered in the system. As mentioned earlier, MHE only uses a finite horizon of latest N measurements to estimate the states; thus, all the discarded previous

measurements that are not included in the current horizon of the MHE problem are considered in a penalty term, referred to as the arrival cost (φ_{k-N}). Note that the MHE stability, the required CPU time, and the accuracy of the solution are highly dependent on the arrival cost (Valipour & Ricardez-Sandoval, 2021).

Once the state estimates are obtained from the solution of problem (4.4), NMPC is engaged to compute the control actions to the RAS such that a high quality of the water is maintained in the fish tanks and fish experience less stress and achieve higher growth. The NMPC layer is explained next.

4.4 Nonlinear Model Predictive Control (NMPC)

As shown in Fig 4.1, NMPC is a receding horizon control that aims to compute a sequence of control actions by solving an optimization problem at each sampling interval k. The control actions are obtained such that the least-squares errors between predicted response of the system and the desired setpoint is minimized over a future horizon (referred to as the prediction horizon) while complying with the process constraints (Mayne et al., 2000; Segovia et al., 2019). Note that the current state of the plant provided by the MHE layer is used as the initial state of the system within the NMPC scheme (Mayne et al., 2000). Therefore, proper initialization of the NMPC optimization problem is key for a smooth closed-loop operation subject to process uncertainty (Valipour & Ricardez-Sandoval, 2022). The NMPC formulation is as follows (Hartley et al., 2012):

$$\min_{\substack{\{x'_i\}_{i=k+1}^{k+P} \\ ,\{u_i\}_{i=k}^{k+C-1}}} \sum_{i=k+1}^{k+P} \left(y'_i - y_{ref}\right)^T \boldsymbol{Q_{CV}} (y'_i - y_{ref}) + \sum_{i=k}^{k+C-1} \Delta u_i{}^T \boldsymbol{Q_{MV}} \Delta u_i \qquad (4.5.A)$$

s.t.

$$x'_{i+1} = F(x'_i, u_i) \qquad \forall\, i = k, \dots, k+P-1 \tag{4.5.B}$$

$$y'_i = H(x'_i, u_i) \qquad \forall\, i = k, \dots, k+P \tag{4.5.C}$$

$$G(x'_i, u_i, y'_i) \leq 0 \qquad \forall\, i = k, \dots, k+P \tag{4.5.D}$$

$$x^l \leq x'_i \leq x^u \qquad \forall\, i = k, \dots, k+P \tag{4.5.E}$$

$$u^l \leq u_i \leq u^u \qquad \forall\, i = k, \dots, k+P \tag{4.5.F}$$

$$u_i = u_{i-1} \qquad \forall\, i = k+C, \dots, k+P \tag{4.5.G}$$

$$\Delta u_i = u_i - u_{i-1} \qquad \forall\, i = k, \dots, k+P \tag{4.5.H}$$

$$x'_i = \widehat{x_k} \qquad \forall\, i = k \tag{4.5.I}$$

where

$x' \in \mathbb{R}^{n_x}, y' \in \mathbb{R}^{n_y}, u \in \mathbb{R}^{n_u}$, $\boldsymbol{Q_{MV}} \in \mathbb{R}^{n_u \times n_u}$, $\boldsymbol{Q_{CV}} \in \mathbb{R}^{n_y \times n_y}$, $x^l \in \mathbb{R}^{n_x}, x^u \in \mathbb{R}^{n_x}$, $u^l \in \mathbb{R}^{n_u}, u^u \in \mathbb{R}^{n_u}$, $F: \mathbb{R}^{n_x \times n_u} \rightarrow \mathbb{R}^{n_x}$, $H: \mathbb{R}^{n_x \times n_u} \rightarrow \mathbb{R}^{n_y}$, $G: \mathbb{R}^{n_x \times n_u \times n_y} \rightarrow \mathbb{R}^{n_g}$

where that x' and y' represents the vectors of predicted states and controlled variables of interest (see Section 4.5) at the i^{th} time interval. Note that there are three different indices indicating time in MHE and NMPC formulations. As mentioned in MHE formulation, index k represents the current time interval of the system (the real time of the plant), whereas index i denotes the time interval within the prediction horizon (i.e., i represents future information and starts from the current time interval k and continues to the future time interval of $k+P$). On the other hand, index j in the MHE formulations represents the time interval within the

moving horizon (i.e., j represents past information and starts from the past time interval $k - N$ and continues to the current time interval k). $\boldsymbol{Q_{CV}}$ and $\boldsymbol{Q_{MV}}$ represent the matrices of the weights on the controlled and manipulated variables, respectively, whereas P and C denote the prediction and control horizon, respectively. The functions F, G, and H used in NMPC formulations are the same as in MHE formulations introduced in the previous section. u_i denotes the control action evaluated by the optimization formulation. Eq. (4.5.G) shows that for prediction horizons larger than the control horizon, the manipulated variables remain constant (equal to the last value in the control horizon) until the end of the prediction horizon. Eq. (4.5.I) represents the relationship between NMPC and MHE.

As illustrated in Fig 4.2, at each time interval k, the RAS update the vector of states (x_k) which may subject to process uncertainties (w_k). Then, the available sensors in the system (which may contain measurement noise (v_k)) update the measurement vector (y_k). After that, MHE uses the plant model together with the available measurements (y_k) to estimate the unmeasurable states and fully reconstruct the vector of system's states crucial for NMPC performance. The output of MHE $(\widehat{x_k})$ is used to initialize NMPC and compute the optimal control actions for the next time interval of the plant $(k + 1)$. These control actions are then sent to the plant to regulate the system towards its setpoint. Time is shifted and this process is repeated for the next time interval.

4.5 Computational experiment

The closed-loop operation of the system along with the implementation of NMPC and MHE is investigated for the RAS system depicted in Fig 4.2. The case study under analysis consists of a

5.5 m^3 fish tank used to grow rainbow trout with the body weight of $45\ gram$. A 40 μm drum filter was used as the mechanical filter to remove large particles whereas two MBBRs, each with the volume of 0.4 m^3, are connected in parallel to the fish tank to remove small particles and dissolved wastes through biological reactions (Fernandes et al., 2017). The specific details of the experimental setup is represented in Table 4.1. The upper/lower limits on the water quality parameters represented through Eq. (4.1) to Eq. (4.3) are shown in Table 4.2 for rainbow trout at 19℃ (the operating temperature of the system). It is expected that fish health is ensured and major losses in fish performance are avoided as long as the water quality parameters satisfy those limits.

Table 4.1

Experimental setup of RAS (data from Fernandes et al. (2017) MBBR trials).

Property	**Value**
Temperature	19℃
Fish body weight	45 g
Fish biomass	130 g
Fish tank volume	5.5 m^3
Biofilter volume	0.4 m^3
Water flow to each biofilter	7.2 m^3/hr

Table 4.2

Allowable limits on water quality parameters at 19℃ (data from Davidson et al., (2014) and Noble (2020)) .

Property	**Value (mg/L)**
DO_{crit}	7
UL_{NH3}	13
UL_{NO3}	75

The closed-loop framework presented in Fig 4.2 was implemented in Pyomo 5.2 in Python 3.6. The RAS model consists of 63 states (i.e., 63 ordinary differential equations) and the backward difference method was used to discretize the nonlinear dynamic model of the system and an interior-point algorithm is used as the solver to the set of differential equations involved in the RAS system. To accommodate the daily fluctuations in the system (e.g. diurnal feed variation) as well as the different time-scales within the system (i.e., fast and slow dynamics of the states involved in the system), the sampling time of the system is set to $0.1\ day$.

To control the present RAS system and provide a good environment for fish growth, concentrations of oxygen ($S_{O,FT}$), ammonia ($S_{NH,FT}$), and nitrate ($S_{NO3,FT}$) in the fish tank are of primary importance and are selected as the controlled variables for the present study. Note that the subscript FT in these variables denote fish tank. The desired values (setpoints) for the oxygen, ammonia, and nitrate concentration are set to $8, 0.62, 21\ mg/L$ respectively. The setpoint for oxygen concentration is selected to be higher than critical oxygen concentration (see Section 3.5.1) so that highest fish growth is achieved. The setpoints for ammonia and nitrate concentration are chosen within the range recommended in the literature to avoid the negative effects of these parameters on fish growth and welfare. The manipulated variables used to maintain the water quality parameters close to their desired values for optimal fish growth are the oxygen flow rate ($m_{O2,FT}$) and make-up water flow rate to the fish tank ($Q_{make-up}$), and the air flow rate to each MBBRs (i.e., $m_{air,MBBR1}, m_{air,MBBR2}$). These variables are the common manipulated variables in the aquaculture and wastewater treatment section (Bian et al., 2017; Fernandes et al., 2017).

A set of scenarios are considered to evaluate the closed-loop performance and implementation of MHE-NMPC framework in the RAS system defined above. The first Scenario (A) compares the closed-loop performance of the system under full access to the states against the case where only a limited number of measurements are available. Scenario B analyzes the closed-loop performance of RAS under an aerator failure in one of the MBBRs whereas Scenario C considers a malfunction of the oxygen probe measuring the oxygen concentration in the fish tanks.

The present study assumes that the process uncertainty associated with each state follows a zero-mean Gaussian distribution with a standard deviation that is set to 0.1% of the nominal steady-state values of the states ($x_{nominal}$). Moreover, there is a zero-mean Gaussian distribution noise with standard deviation of $1e-6\ x_{nominal}$ associated with each of the measurement devices. Note that the nominal values of the states were obtained through open-loop tests assuming a continuous feeding rate of $2kg/day$. Nominal values for $Q_{make-up}$, $m_{O2,FT}$, $m_{air,MBBR1}$, $and\ m_{air,MBBR2}$ were set to $3m^3/day$, $1.04\ kg/day$, $0.6m^3/day$, $0.6m^3/day$ respectively.

At the initial time (i.e., $t = 0$), the NMPC is engaged within the plant and the feed is only allocated daily for a 6-hour period, with the rate of $3\ kg/day$. Moreover, the prediction and control horizon for NMPC controller in this study are equal and set to 5 days; these values were found to provide good control performance in terms of fast response in achieving the setpoint while avoiding aggressive control actions. To drive the system to their set points, the first term in the objective function in problem (4.5) is weighted by $\boldsymbol{Q_{CV}} = diag(500,100,100)$ for oxygen, ammonia and nitrate concentration, respectively. Similarly, to avoid drastic changes in the

manipulative variables, the second term in the objective function in problem (4.5) is weighted $\boldsymbol{Q_{MV}} = diag(0.001,0.0001,0.0001,0.0001)$ for $Q_{make-up}$, $m_{O2,FT}$, $m_{air,MBBR1}$, $m_{air,MBBR2}$, respectively. Note that the arrival cost in the MHE formulation has not been considered in this study. As a result, the length of estimation horizon (N) is set to a relatively large number to mitigate the effect of arrival cost (N = 15). This horizon was selected through preliminary closed-loop tests and was found to be long enough to estimate states with a reasonable accuracy at acceptable computational costs.

The performance of the closed-loop is evaluated through calculation of sum of squared errors (SSE) between the controlled variables and their corresponding setpoints, i.e.,

$$SSE = \frac{1}{n'}\sum_{k'=1}^{n}(y_{k'} - y_{ref})^2 \quad (4.6)$$

where n' represents the number of sampling intervals in the given scenario, $y_{k'}$ is the controlled variable for sample k' whereas y_{ref} represents the desired setpoint for the controlled variable of interest.

4.5.1 Scenario A: Closed-loop operation of RAS under full and partial access to the states

The closed-loop performance of RAS under full and partial access to the states is evaluated in this Scenario. Instance A1 evaluates the closed-loop operation of RAS under full access to the states whereas Instance A2 assumes that only a limited number of states are measured online. In both instances the measurements are subject to a zero-mean Gaussian distribution noise with standard deviation of $1e-6\ x_{nominal}$. The available measurements in the system (the fish tank and in the two biological reactors (MBBR1 and MBBR2)) for Instance A2 are given in

Table 4.3 (notation is provided in the nomenclature). Note that it is assumed that concentration of oxygen, ammonia, nitrite, nitrate, COD, and BOD can be measured online through the available commercial equipment in the market (Busch et al., 2013). In the case of bacteria, in addition to the measurements in the bulk, it is assumed that the online measurement of the bacteria concentration ($AOB, NOB, and\ het$) in the biofilm is also available. Although online measurement of bacteria is less common, Højris et al., (2016) presented a rapid, chemical-free method for on-line monitoring of non-specific bacteria in water, based on 3D scanning by a moving digital microscope; thus indicating brighter future in online measurements of water quality parameters in RAS.

Table 4.3

Available measurements of the system for Instance A2.

Measurement	Fish tank	MBBR1 (bulk)	MBBR2 (bulk)	MBBR1 (biofilm)	MBBR2 (biofilm)
O_2	✓	✓	✓		
NH_3	✓	✓	✓		
NO_2	✓	✓	✓		
NO_3	✓	✓	✓		
COD	✓	✓	✓		
BOD	✓	✓	✓		
AOB		✓	✓	✓	✓
NOB		✓	✓	✓	✓
Het		✓	✓	✓	✓

$COD = S_S + X_S + S_I + X_I + X_{AOB} + X_{NOB} + X_H$

$BOD = S_S + X_S$ (Busch et al., 2013)

The results for oxygen concentration for Instances A1 and A2 are shown in Fig. 4.3. Due to the feeding regime selected (i.e., fish are only fed for a 6-hour period everyday), there is a diurnal variation in the concentration of oxygen, i.e., after the feeding, the oxygen concentration decreases whereas as feeding stops, the oxygen concentration increases. Despite this diurnal variation observed in the concentration of oxygen in both cases, as it is illustrated in Fig 4.3, the controller aims to maintain the oxygen concentration at the given setpoint ($8\ mg/L$) within each feeding cycle (see inner plots shown in Fig 4.3). Moreover, the oxygen concentration is kept above the critical value of oxygen at all times (DO_{crit} is $7\ mg/L$ at the operating temperature of the system) except for the short period in the beginning caused by the transient behavior of the system due to changes in the feeding rate and feeding regime, i.e., feeding changes from a continuous regime with the rate of $2\ kg/day$ under open-loop operation to a 6-hour period regime with the rate of $3\ kg/day$ under closed-loop. Note that this short time exposure to oxygen concentrations lower than $7\ mg/L$ will not have severe or long lasting effects on rainbow trout welfare (Noble, 2020).

To compare the closed-loop performance of the system under partial and full access to the states, the SSE for ammonia, oxygen, and nitrate (the controlled variables of concern) were computed and are listed in Table 4.4. As shown in this Table, the SSE for ammonia is almost the same for Instance A1 and A2. However, the SSE for oxygen and nitrate under partial access is 37% and 48% higher than the SSE under full access respectively, representing that closed-loop performance is negatively affected for Instance A2 (under partial access to the states). The difference in SSE is better illustrated for oxygen in the zoomed in profiles of Fig 4.3 through the observed offset (Instance A1 has lower offset than the Instance A2). This difference results from

the limitations in the available number of measurements of the system in Instance A2. Note that, although Instance A1 represents a better performance in setpoint tracking and SSE error; the assumption of full accessibility to the states is not realistic in the aquaculture farms due to the limitations in the measurement devices; thus, Instance A2 represents a more practical situation for closed-loop operation of RAS. Moreover, despite the higher SSE in Instance A2, the oxygen concentration is still maintained within the range compatible with rainbow trout needs thus ensuring fish well-being.

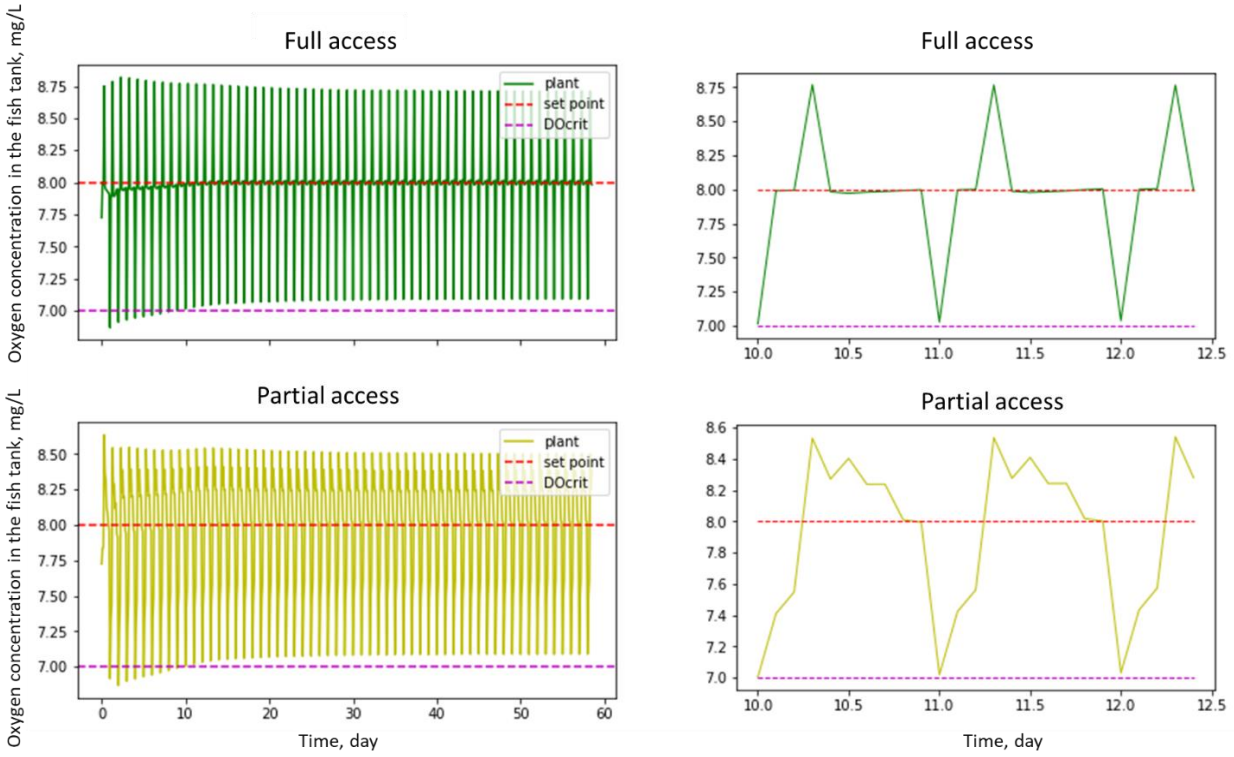

Fig 4.3 Oxygen concentration under full (top) and partial (bottom) access to the states (left: full profile, right: zoomed in profile).

Table 4.4

Comparison of SSE for ammonia, oxygen, and nitrate under full and partial access to the states.

Controlled variable	Instance A1 (full access)	Instance A2 (partial access)
Ammonia	1.12812e-07	1.12814e-07
Oxygen	1.43168e-07	1.95760e-07
Nitrate	1.64429e-08	2.43006e-08

Concentration of ammonia and nitrate together with the manipulated variables in the system under partial access to the states (Instance A2) are shown in Fig 4.4. Although nitrate concentration fluctuates around its setpoint ($21\ mg/L$), the ammonia concentration is always lower than the selected setpoint ($0.62\ mg/L$). This behavior can be explained by the weight matrix in the NMPC objective function. Note that among the three controlled variables, oxygen is the most critical water quality parameter, therefore a higher weight is assigned to this variable (500 for oxygen vs. 100 for both ammonia and nitrate) to keep its concentration on target. In the case of ammonia and nitrate concentrations; as long as the concentration of these variables remain below their toxic levels ($13\ mg/L$ and $75\ mg/L$ respectively), fish health is not negatively affected and thus there is no need for these variables to strictly follow a setpoint.

As shown in Fig 4.4, the manipulative variables of the system fluctuate daily to accommodate the diurnal variations in the feeding regime. As feeding starts, the concentration of waste components increases in the system whereas the concentration of oxygen decreases. Accordingly, the make-up water flow rate as well as $m_{O2,FT}$, $m_{air,MBBR1}$, $and\ m_{air,MBBR2}$ increase to reduce waste concentration and increase dissolved oxygen within the system. As feeding stops, the opposite trend is observed in the manipulative variables. Note that providing

sufficient oxygen in water is not only important for fish but it is also essential for the nitrification since this process depends strongly on the oxygen availability in the system (Piculell et al., 2016). Therefore, the increase in $m_{O2,FT}$, $m_{air,MBBR1}$, $and\ m_{air,MBBR2}$ to keep oxygen concentration on target is twofold: 1) to maintain fish well-being, 2) to ensure proper nitrification and thus effective ammonia removal in the system.

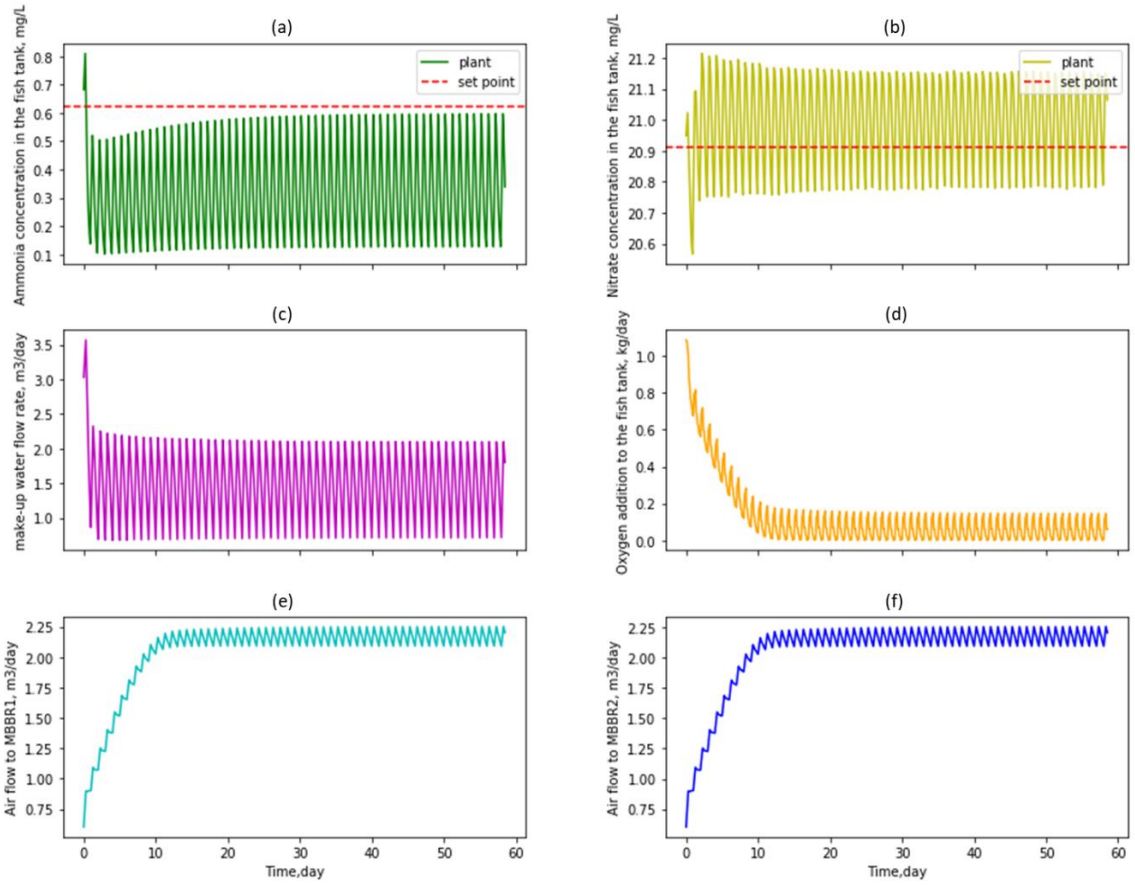

Fig 4.4 Controlled variables (a, b), and manipulated variables (c - f) under partial access to the states (Instance A2).

4.5.2 Scenario B: Aerator failure in MBBR2

In this scenario, the closed-loop performance of RAS is assessed under the case where the aerator delivering air to the MBBR2 fails for a period of one week; from day 10 to day 17 (for the period of aerator failure, $m_{air,MBBR2} = 0$). The operating conditions and all the other assumptions (including the feeding rate) are the same as those presented in Section 4.5. Moreover, the available measurements are similar to that shown in Table 4.3. The results of this scenario are shown in Fig 4.5.

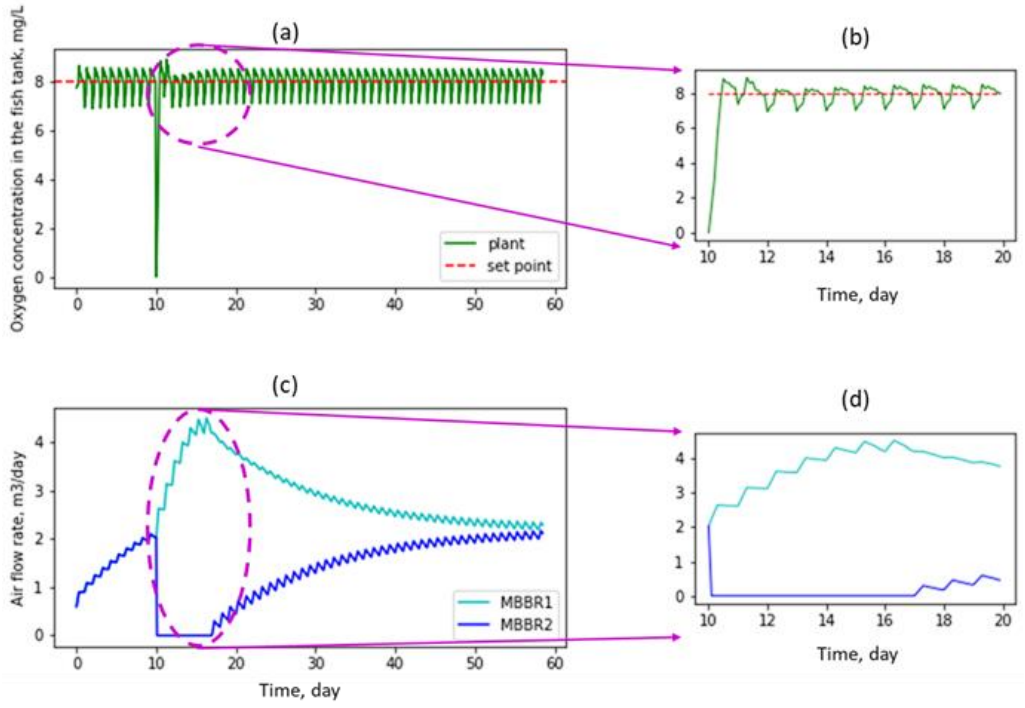

Fig 4.5 Concentration of oxygen in the fish tank as well as air flow rate to MBBRs (a,c: full profile, b,d: zoomed in profile) under failure in MBBR2 aerator (Scenario B).

As shown in Fig 4.5, following the failure in the MBBR2 aerator, the oxygen concentration drops suddenly to zero; this situation in the absence of backup oxygen supply causes major losses in

the system due to high stocking densities and low water exchange rate in RAS. Therefore, presence of emergency oxygen backups is fundamental for fish well-being and profitability of the system (Timmons et al., 2002). However, despite the failure of the aerator and the resulting low oxygen concentration in the system, as shown in the right-hand side plot of Fig 4.5, the NMPC brings the oxygen concentration back to values higher than $7\ mg/L$ and keeps it within the acceptable range for rainbow trout at all times through increasing the air flow rate in MBBR1. Note that under the period of the aerator's malfunction, the aerator in MBBR1 is the main oxygen supplier in the system and thus there is an increasing trend in the flow rate of this aerator. However, as the aerator in MBBR2 resumes to normal operation, since MBBR1 will no longer be the only oxygen supplier, the air flow rate in MBBR1 decreases while the air flow in MBBR2 increases.

The closed-loop framework showed acceptable performance in adjusting the oxygen concentration during the failure of the aerator; however, the presence of back-up oxygen supply is of high priority and should not be underestimated. For instance, in the absence of oxygen backups, oxygen concentration can drop to stressful levels for fish in approximately 60 minutes in a moderately stocked (60 kg/m^3) RAS or within 10 minutes in a highly stocked (120 kg/m^3) warmwater system (Tidwell, 2012).

4.5.3 Scenario C: Malfunction of the oxygen probe in the fish tank

In this scenario, closed-loop performance of RAS is assessed under the case where there is a temporary malfunction in the oxygen probe measuring the oxygen concentration in the fish tank for a period of one week (from day 10 to day 17). During this period, the oxygen probe is

subject to a zero-mean Gaussian distribution noise with a standard deviation that is set to 10% of the nominal steady-state value of the state (oxygen concentration) in the fish tank. Note that for this scenario, process and measurement noises for all the other states is the same as in Instance A2 in Scenario A. The operating conditions and all the other assumptions considered for this scenario (including the feeding rate) are similar to the assumptions listed in Section 4.5. The available measurements in this scenario follow Table 4.3. The results for Scenario C are shown in Fig 4.6.

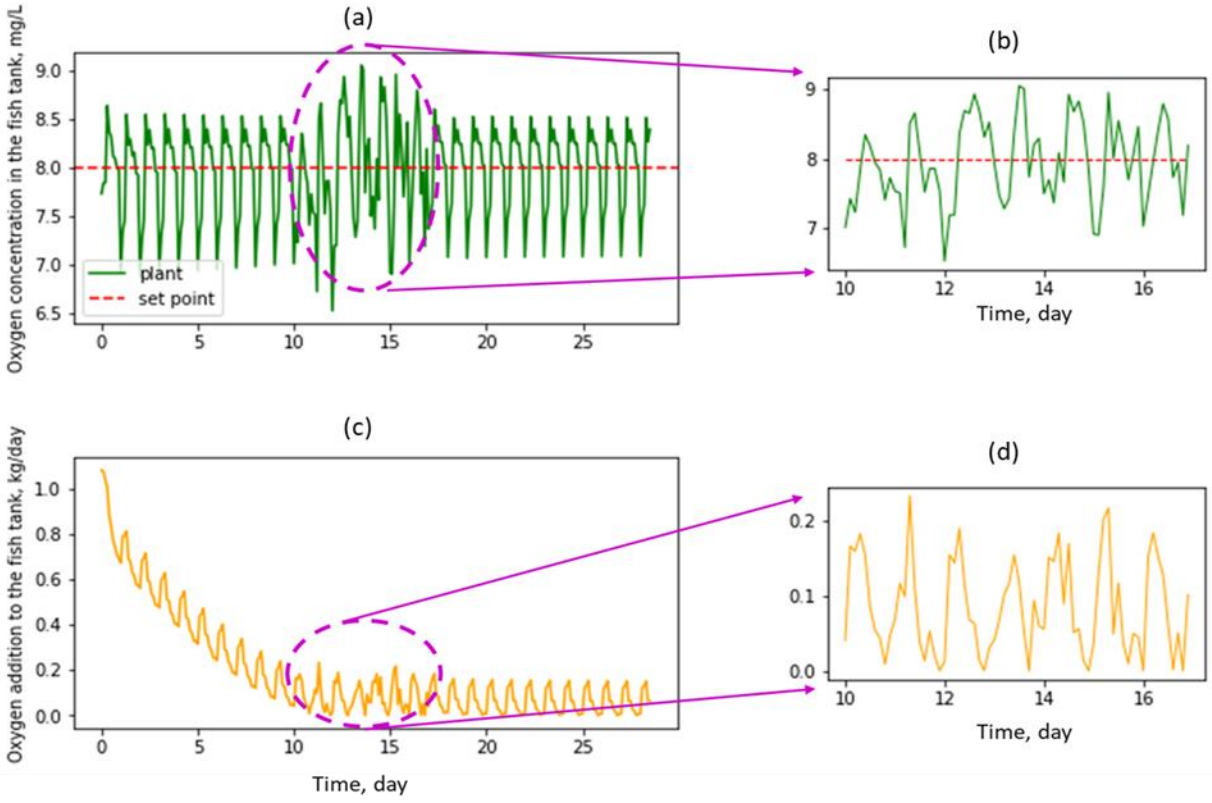

Fig 4.6 Oxygen concentration as well as oxygen addition rate to the fish tank (a,c: full profile, b,d: zoomed in profile) under malfunction of the oxygen probe (Scenario C).

As shown in Fig 4.6, during the oxygen probe malfunction, the fluctuations in the oxygen concentration are accentuated due to the noisy measurements produced by the oxygen probe.

However, as shown in the right-hand side plot of Fig 4.6, even in the presence of these noisy measurements, the controller is able to keep the oxygen concentration close to the setpoint ($8\ mg\ /L$) through changes in $m_{O2,FT}$. Nevertheless, at some points during this period, the oxygen concentration drops below the critical value ($7\ mg\ /L$); however, since the exposure time to low oxygen concentrations is relatively short, fish welfare is not affected.

4.6 Summary

To grow healthy fish, increase fish growth, and improve survival rate, the quality of the water in the rearing environment should be carefully controlled. For this purpose, application of advanced MIMO controllers capable of handling interactive, nonlinear behavior of RAS is fundamental in keeping multiple critical water quality parameters on target simultaneously and thus avoiding major losses in the system. To this aim, an integrated closed-loop approach involving advanced model-based state estimation and control systems such as MHE and NMPC was implemented to analyze the closed-loop performance of the system under typical scenarios that may emerge during the operation of RAS. In the first scenario, the closed-loop framework was tested under full and partial access to the states. According to the results, even under partial access to the states (a common scenario in the operation of RAS due to the limitations of the measurement devices), the closed-loop performance of the system is not affected significantly. That is, the water quality parameters (concentration of ammonia, oxygen, and nitrate) are maintained within the acceptable levels for rainbow trout. Moreover, the proposed closed-loop framework can maintain the quality of the water in accordance with fish needs

even under sensor malfunction (oxygen probe in the fish tank) or failure of a unit (aerator crash). However, the presence of emergency oxygen backup is inevitable in RAS so that intense fish mortalities are avoided under critical situations which may happen during the actual operation.

Overall, the closed-loop framework used in this study demonstrated high potential for the application of advanced model-based state estimation and control systems for the closed-loop operation of RAS since they are able to provide a good environment that can lead to a reduction in fish mortality, higher growth rate, and healthier fish.

Chapter 5

Conclusions and Recommendations

RAS is an environmentally friendly fish production method that was developed to overcome the shortcomings of the traditional fish farming methods (e.g. cages or raceways) such as high-water consumption and waste discharge through addition of a treatment section. This being said, to maintain the quality of the water in accordance with fish requirements, the fish tank effluents should pass through mechanical and biological filtrations as well as oxygen addition units before returning back to the fish tanks. However, as a recent innovative technology, more studies are needed for in-depth understanding of RAS with the goal of better management and effective operation of these system. The first objective of this thesis was to develop a dynamic model of RAS using a modular approach. That is, the major units of RAS (i.e., fish tank, mechanical filter, biological reactor) were modeled individually and were then integrated through material streams to build the entire RAS system. The major advantage of this approach is that the existing units can be easily removed/replaced with other units based on a specific application or designer's preferences. Note that the rearing environment has a major influence on fish performance in terms of growth and mortality; however, these underlying interactions have not been considered in the literature. In this work, growth and mortality relations were explicitly incorporated within the proposed RAS model to reflect the effect of water quality parameters on fish well-being. The proposed model was then validated using the available data in the literature for a rainbow trout RAS system with the fish tank volume of 5.5 m^3 and initial stocking density of 24 kg/m^3. This model was later used to assess fish performance under

different management strategies in terms of feeding regime and degree of water recirculation (the ratio of make-up flow rate to feeding rate) to provide insights regarding the operation and management of these systems. Results from this study showed that continuous feeding leads to less fluctuations in the fish tank effluents, which is important in waste management and sizing of the treatment section. Moreover, the degree of water recirculation should be kept as low as possible to reduce water consumption in RAS; however, the results also indicated that for values below 0.06, the nitrate concentration can reach to toxic values (e.g., > 600 mg/L). To avoid nitrate accumulation, the addition of denitrification units would be necessary in RAS.

The second part of this thesis focused on closed-loop performance of RAS through implementation of MHE-NMPC framework that aims to maintain the water quality parameters on target. The performance of the proposed control methodology was investigated in the presence of process uncertainty and measurement noises under full accessibility to the states. The results of this scenario showed satisfactory performance in maintaining the key controlled variables near their setpoints (i.e., ammonia, oxygen, and nitrate concentrations). The performance of the system was also evaluated under partial access to the states, which is a common scenario in the operation of RAS due to the limitations on accessibility to key states of the system. Based on the results, the control performance was negatively affected under partial access. Since the performance of NMPC controller highly depends on full accessibility to the states, the tracking errors for the controlled variables under partial access were higher than those obtained for the case of full access (e.g., the tracking errors were 37% and 48% higher for oxygen and nitrate concentrations under partial access compared to full access, respectively). Despite these errors under partial accessibility to the states, the water quality parameters

remained within the range compatible with fish needs thus demonstrating the capability of the proposed control scheme. The proposed closed-loop framework was also assessed under realistic scenarios that are likely to happen in the operation of RAS, such as failure of the aerator in one of the MBBR and malfunction of the sensor measuring the oxygen concentration in the system. In both scenarios, the proposed scheme was able to keep the water quality parameters close to their desired setpoints. However, despite the capability of the proposed control scheme, the application of emergency suppliers (e.g., oxygen backup) is important to avoid major losses in the system. Overall, the MHE-NMPC framework proposed in this study demonstrated high potential in closed-loop operation of RAS since it can deliver an environment for fish that can lead to higher growth rate, lower mortalities, and healthier fish.

5.1 Recommendations for future research

The main recommendations that can motivate the future works in this emerging field are as follows:

- The validation of the model was considered using the experimental data available in the literature for a small RAS system with the fish tank volume of 5.5 m^3 and initial stocking density of 24 kg/m^3. Note that further validation of the model for larger RAS systems with higher capacities has not been considered in this work due to the scarcity of the data in the literature. Moreover, most of the current experimental studies available for pilot-scale RAS do not include all the information needed for verification and validation. Therefore, future work should consider further validation of the proposed model for large-scale RAS systems as new experimental data emerge in the literature.

- The particular RAS design used in this study can be further expanded such that it involves multiple rearing tanks and/or additional wastewater treatment units such as denitrification (used for nitrate removal) or carbon dioxide removal units. Future studies can consider these alternative designs to increase fish production rates or meet specific regulations (e.g., maintain low concentration of nitrate in water).
- The dynamic RAS model proposed in this work only considered mass balances in modeling of RAS. However, temperature is another important water quality parameter that can affect fish performance and needed to be carefully controlled. Consequently, a thermal analysis of the system through coupling of the mass and energy balances is another area of future research that may lead to better prediction and control in RAS. Upon addition of energy balances, the performance of the proposed MHE-NMPC framework should be re-assessed for temperature control in the RAS to investigate the capability of the proposed framework.
- In this study, it was assumed that fish growth was uniform (i.e., there is no size variation among fish individuals in a rearing tanks). Variation in growth is a common feature of fish population that can induce the suppressive influence of large fish on small fish (Barki et al., 2000). Size grading (sorting of fish into different groups with similar size) is a method to reduce the non-uniformity in fish sizes as well as the negative impacts associated with that. As a future work, the fish growth model used in this study can be modified such that it accounts for this size variation. The addition of such a growth model may be a more realistic representation of the RAS that can be further used to determine the time required between grading.

- Integration of design and control is another future area of research for RAS systems. Typically, process design is performed using only steady-state information followed by a controllability analysis that takes into account the process dynamics. It has been shown that this approach may lead to infeasible designs (Rafiei and Ricardez-Sandoval, 2020). Integration of design and control have emerged as an alternative to determine process design decisions while taking into account the operation of the system in closed-loop. In the integrated approach, the trade-off between the conflicting objectives of steady-state economics and dynamic performance can lead to optimal designs while ensuring feasible operation of the process under different disruptions/disturbances in the system (Rafiei & Ricardez-Sandoval, 2018). To date, integration of design and control for RAS systems has not been attempted. It is expected that advanced integration of design and control techniques (e.g., Palma-Flores & Ricardez-Sandoval, 2022; Rafiei & Ricardez-Sandoval, 2020b) would return attractive RAS designs that can ensure the closed-loop dynamic feasibility of the system at minimum cost
- The application of machine learning in aquaculture is another future area of research for RAS. This technology can be used in the biomass detection (e.g., estimation of fish size, weight, and number), recognition and classification of fish (e.g., age and sex identification), behavioral analysis (e.g., feeding and fish group behavior) and prediction of water quality parameters (e.g., dissolved oxygen content) (Zhao et al., 2021). The application of machine learning technology for RAS may lead to effective management of aquaculture plants, scientific breeding, control of reproduction density, identifying breeding biological

anomalies, preventing diseases and reducing corresponding risks (Zhao et al., 2021) and to reduce energy consumption from this plant (Rangel-Martinez et al., 2021).

REFERENCES

Ahmad, A., Sheikh Abdullah, S. R., Hasan, H. A., Othman, A. R., & Ismail, N. 'Izzati. (2021). Aquaculture industry: Supply and demand, best practices, effluent and its current issues and treatment technology. Journal of Environmental Management, 287, 112271. https://doi.org/10.1016/j.jenvman.2021.112271

Albertos, P., Sala, A., & Olivares, M. (2000, September 20). Fuzzy Logic Controllers. Methodology, Advantages and Drawbacks. https://doi.org/10.13140/RG.2.1.2512.6164

Alexander, R., Campani, G., Dinh, S., & Lima, F. V. (2020). Challenges and Opportunities on Nonlinear State Estimation of Chemical and Biochemical Processes. Processes, 8(11), 1462. https://doi.org/10.3390/pr8111462

Almeida, P., Dewasme, L., & Vande Wouwer, A. (2020). Denitrification Control in a Recirculating Aquaculture System—A Simulation Study. Processes, 8(10), 1306. https://doi.org/10.3390/pr8101306

Andreottola, G., Foladori, P., Ragazzi, M., & Tatàno, F. (2000). Experimental comparison between MBBR and activated sludge system for the treatment of municipal wastewater. Water Science and Technology, 41(4–5), 375–382. https://doi.org/10.2166/wst.2000.0469

Ansari, F. A., Guldhe, A., Gupta, S. K., Rawat, I., & Bux, F. (2021). Improving the feasibility of aquaculture feed by using microalgae. Environmental Science and Pollution Research, 28(32), 43234–43257. https://doi.org/10.1007/s11356-021-14989-x

Badiola, M., Mendiola, D., & Bostock, J. (2012). Recirculating Aquaculture Systems (RAS) analysis: Main issues on management and future challenges. Aquacultural Engineering, 51, 26–35.

Barki, A., Harpaz, S., Hulata, G., & Karplus, I. (2000). Effects of larger fish and size grading on growth and size variation in fingerling silver perch. Aquaculture International, 8(5), 391–401. https://doi.org/10.1023/A:1009274726380

Bassin, J. P., Dias, I. N., Cao, S. M. S., Senra, E., Laranjeira, Y., & Dezotti, M. (2016). Effect of increasing organic loading rates on the performance of moving-bed biofilm reactors filled with different support media: Assessing the activity of suspended and attached biomass fractions. Process Safety and Environmental Protection, 100, 131–141. https://doi.org/10.1016/j.psep.2016.01.007

Bian, W., Zhang, S., Zhang, Y., Li, W., Kan, R., Wang, W., Zheng, Z., & Li, J. (2017). Achieving nitritation in a continuous moving bed biofilm reactor at different temperatures through ratio control. Bioresource Technology, 226, 73–79. https://doi.org/10.1016/j.biortech.2016.12.014

Bregnballe, J., Eurofish International Organisation, C., & Fao, B. (2010). A guide to recirculation aquaculture: An introduction to the new environmentally friendly and highly productive closed fish farming systems. Copenhagen (Denmark) Eurofish/FAO Subregional Office for Central and Eastern Europe. https://scholar.google.com/scholar_lookup?title=A+guide+to+recirculation+aquaculture%3A+an+introduction+to+the+new+environmentally+friendly+and+highly+productive+closed+fish+farming+systems&author=Bregnballe%2C+J.&publication_year=2010

Bureau, D. P., & Hua, K. (2010). Towards effective nutritional management of waste outputs in aquaculture, with particular reference to salmonid aquaculture operations. Aquaculture Research, 41(5), 777–792. https://doi.org/10.1111/j.1365-2109.2009.02431.x

Busch, J., Elixmann, D., Kühl, P., Gerkens, C., Schlöder, J. P., Bock, H. G., & Marquardt, W. (2013). State estimation for large-scale wastewater treatment plants. Water Research, 47(13), 4774–4787. https://doi.org/10.1016/j.watres.2013.04.007

Camargo, J. A., Alonso, A., & Salamanca, A. (2005). Nitrate toxicity to aquatic animals: A review with new data for freshwater invertebrates. Chemosphere, 58(9), 1255–1267. https://doi.org/10.1016/j.chemosphere.2004.10.044

Chahid, A., N'Doye, I., Majoris, J. E., Berumen, M. L., & Laleg-Kirati, T. M. (2021). Model predictive control paradigms for fish growth reference tracking in precision aquaculture. Journal of Process Control, 105, 160–168. https://doi.org/10.1016/j.jprocont.2021.07.015

Chen, S., Timmons, M. B., Aneshansley, D. J., & Bisogni, J. J. (1993). Suspended solids characteristics from recirculating aquacultural systems and design implications. Aquaculture, 112(2), 143–155. https://doi.org/10.1016/0044-8486(93)90440-A

Davidson, J., Good, C., Welsh, C., & Summerfelt, S. T. (2014). Comparing the effects of high vs. Low nitrate on the health, performance, and welfare of juvenile rainbow trout Oncorhynchus mykiss within water recirculating aquaculture systems. Aquacultural Engineering, 59, 30–40. https://doi.org/10.1016/j.aquaeng.2014.01.003

Davidson, J., & Summerfelt, S. (2004). Solids flushing, mixing, and water velocity profiles within large (10 and 150 m3) circular 'Cornell-type' dual-drain tanks. Aquacultural Engineering, 32(1), 245–271. https://doi.org/10.1016/j.aquaeng.2004.03.009

FAO. (2020). The State of World Fisheries and Aquaculture 2020: Sustainability in action. FAO. https://doi.org/10.4060/ca9229en

Farghally, H. M., Atia, D. M., El-madany, H. T., & Fahmy, F. H. (2014). Control methodologies based on geothermal recirculating aquaculture system. Energy, 78, 826–833. https://doi.org/10.1016/j.energy.2014.10.077

Fernandes, P. M., Pedersen, L.-F., & Pedersen, P. B. (2017). Influence of fixed and moving bed biofilters on micro particle dynamics in a recirculating aquaculture system. Aquacultural Engineering, 78, 32–41. https://doi.org/10.1016/j.aquaeng.2016.09.002

Fowler, P., Baird, D., Bucklin, R., Yerlan, S., Watson, C., & Chapman, F. (1994). Microcontrollers in recirculating aquaculture systems. EES (USA). https://scholar.google.com/scholar_lookup?title=Microcontrollers+in+recirculating+aquaculture+systems&author=Fowler%2C+P.+%28University+of+Florida.%29&publication_year=1994

Han, H., & Qiao, J. (2014). Nonlinear Model-Predictive Control for Industrial Processes: An Application to Wastewater Treatment Process. IEEE Transactions on Industrial Electronics, 61(4), 1970–1982. https://doi.org/10.1109/TIE.2013.2266086

Hartley, E. N., Trodden, P. A., Richards, A. G., & Maciejowski, J. M. (2012). Model predictive control system design and implementation for spacecraft rendezvous. Control Engineering Practice, 20(7), 695–713. https://doi.org/10.1016/j.conengprac.2012.03.009

Højris, B., Christensen, S. C. B., Albrechtsen, H.-J., Smith, C., & Dahlqvist, M. (2016). A novel, optical, on-line bacteria sensor for monitoring drinking water quality. Scientific Reports, 6, 23935. https://doi.org/10.1038/srep23935

Jie, C., Yingying, S., Junhui, W., Yusheng, W., Huiping, S., & Kaiyan, L. (2019). Intelligent Control and Management System for Recirculating Aquaculture. 2019 IEEE 2nd International Conference on Electronics and Communication Engineering (ICECE), 438–443.

Karimanzira, D., Keesman, K. J., Kloas, W., Baganz, D., & Rauschenbach, T. (2016). Dynamic modeling of the INAPRO aquaponic system. Aquacultural Engineering, 75, 29–45. https://doi.org/10.1016/j.aquaeng.2016.10.004

Kawan, J., Abu Hasan, H., Suja, F., Jaafar, O., & Abd-Rahman, R. (2016). A review on sewage treatment and polishing using moving bed bioreactor (Mbbr). 11, 1098–1120.

Kermani, M., Bina, B., Movahedian, H., Amin, M. M., & Nikaein, M. (2008). Application of Moving Bed Biofilm Process for Biological Organics and Nutrients Removal from Municipal Wastewater.

American Journal of Environmental Sciences, 4(6), 675–682. https://doi.org/10.3844/ajessp.2008.675.682

Lee, P. G., Lea, R. N., Dohmann, E., Prebilsky, W., Turk, P. E., Ying, H., & Whitson, J. L. (2000). Denitrification in aquaculture systems: An example of a fuzzy logic control problem. Aquacultural Engineering, 23(1), 37–59. https://doi.org/10.1016/S0144-8609(00)00046-7

Losordo, T., & Hobbs, A. (2000). Using computer spreadsheets for water flow and biofilter sizing in recirculating aquaculture production systems. Aquacultural Engineering, 23, 95–102. https://doi.org/10.1016/S0144-8609(00)00048-0

Martins, C. I. M., Eding, E. H., Verdegem, M. C. J., Heinsbroek, L. T. N., Schneider, O., Blancheton, J. P., d'Orbcastel, E. R., & Verreth, J. A. J. (2010). New developments in recirculating aquaculture systems in Europe: A perspective on environmental sustainability. Aquacultural Engineering, 43(3), 83–93. https://doi.org/10.1016/j.aquaeng.2010.09.002

Mayne, D. Q., Rawlings, J. B., Rao, C. V., & Scokaert, P. O. M. (2000). Constrained model predictive control: Stability and optimality. Automatica, 36(6), 789–814. https://doi.org/10.1016/S0005-1098(99)00214-9

Noble, E. C. (2020). Welfare Indicators for farmed rainbow trout: Tools for assessing fish welfare. 311.

Ostace, G., Cristea, V., & Agachi, P. (2011). Extension of activated sludge model no 1 with two-step nitrification and denitrification processes for operation improvement. Environmental Engineering and Management Journal, 10, 1529–1544. https://doi.org/10.30638/eemj.2011.214

Palma-Flores, O., & Ricardez-Sandoval, L. A. (2022). Integration of design and NMPC-based control for chemical processes under uncertainty: An MPCC-based framework. Computers & Chemical Engineering, 162, 107815. https://doi.org/10.1016/j.compchemeng.2022.107815

Pedersen, S. (2018). Simulation and Optimization of Recirculating Aquaculture Systems [Chalmers University of Technology]. https://research.chalmers.se/en/publication/505266

Piculell, M., Welander, P., Jönsson, K., & Welander, T. (2016). Evaluating the effect of biofilm thickness on nitrification in moving bed biofilm reactors. Environmental Technology, 37(6), 732–743. https://doi.org/10.1080/09593330.2015.1080308

Piculell, M., Welander, T., & Jönsson, K. (2013). Organic removal activity in biofilm and suspended biomass fractions of MBBR systems. Water Science and Technology, 69(1), 55–61. https://doi.org/10.2166/wst.2013.552

Rafiei, M., & Ricardez-Sandoval, L. A. (2018). Stochastic Back-Off Approach for Integration of Design and Control Under Uncertainty. Industrial & Engineering Chemistry Research, 57(12), 4351–4365. https://doi.org/10.1021/acs.iecr.7b03935

Rafiei, M., & Ricardez-Sandoval, L. A. (2020a). New frontiers, challenges, and opportunities in integration of design and control for enterprise-wide sustainability. Computers & Chemical Engineering, 132, 106610. https://doi.org/10.1016/j.compchemeng.2019.106610

Rafiei, M., & Ricardez-Sandoval, L. A. (2020b). Integration of design and control for industrial-scale applications under uncertainty: A trust region approach. Computers & Chemical Engineering, 141, 107006. https://doi.org/10.1016/j.compchemeng.2020.107006

Rangel-Martinez, D., Nigam, K. D. P., & Ricardez-Sandoval, L. A. (2021). Machine learning on sustainable energy: A review and outlook on renewable energy systems, catalysis, smart grid and energy storage. Chemical Engineering Research and Design, 174, 414–441. https://doi.org/10.1016/j.cherd.2021.08.013

Remen, M., Sievers, M., Torgersen, T., & Oppedal, F. (2016). The oxygen threshold for maximal feed intake of Atlantic salmon post-smolts is highly temperature-dependent. Aquaculture, 464, 582–592. https://doi.org/10.1016/j.aquaculture.2016.07.037

Ross, R. M., & Watten, B. J. (1998). Importance of rearing-unit design and stocking density to the behavior, growth and metabolism of lake trout (Salvelinus namaycush). Aquacultural Engineering, 19(1), 41–56. https://doi.org/10.1016/S0144-8609(98)00041-7

Sapkota, A., Sapkota, A. R., Kucharski, M., Burke, J., McKenzie, S., Walker, P., & Lawrence, R. (2008). Aquaculture practices and potential human health risks: Current knowledge and future priorities. Environment International, 34(8), 1215–1226. https://doi.org/10.1016/j.envint.2008.04.009

Segovia, P., Rajaoarisoa, L., Nejjari, F., Duviella, E., & Puig, V. (2019). Model predictive control and moving horizon estimation for water level regulation in inland waterways. Journal of Process Control, 76, 1–14. https://doi.org/10.1016/j.jprocont.2018.12.017

Sehar, S., & Naz, I. (2016). Role of the Biofilms in Wastewater Treatment. In Microbial Biofilms—Importance and Applications. IntechOpen. https://doi.org/10.5772/63499

Shinn, A. P., Pratoomyot, J., Griffiths, D., Trong, T. Q., Vu, N. T., Jiravanichpaisal, P., & Briggs, M. (2018). Asian shrimp production and the economic costs of disease.

Tidwell, J. H. (2012). Aquaculture Production Systems. John Wiley & Sons.

Timmons, M., Ebeling, J., Wheaton, F. W., Summerfelt, S., & Vinci, B. (2002). Recirculating Aquaculture System.

Valipour, M., & Ricardez-Sandoval, L. A. (2021). Assessing the Impact of EKF as the Arrival Cost in the Moving Horizon Estimation under Nonlinear Model Predictive Control. Industrial & Engineering Chemistry Research, 60(7), 2994–3012. https://doi.org/10.1021/acs.iecr.0c06095

Valipour, M., & Ricardez-Sandoval, L. A. (2022). Extended moving horizon estimation for chemical processes under non-Gaussian noises. AIChE Journal, 68(3), e17545. https://doi.org/10.1002/aic.17545

Valipour, M., Toffolo, K. M., & Ricardez-Sandoval, L. A. (2021). State estimation and sensor location for Entrained-Flow Gasification Systems using Kalman Filter. Control Engineering Practice, 108, 104702. https://doi.org/10.1016/j.conengprac.2020.104702

van Rijn, J., Tal, Y., & Schreier, H. J. (2006). Denitrification in recirculating systems: Theory and applications. Aquacultural Engineering, 34(3), 364–376. https://doi.org/10.1016/j.aquaeng.2005.04.004

Vielma, J., Kankainen, M., & Setälä, J. (2021). Current status of recirculation aquaculture systems (RAS) and their profitability and competitiveness in the Baltic Sea area. 30.

Wik, T. E. I., Lindén, B. T., & Wramner, P. I. (2009). Integrated dynamic aquaculture and wastewater treatment modelling for recirculating aquaculture systems. Aquaculture, 287(3), 361–370. https://doi.org/10.1016/j.aquaculture.2008.10.056

Zhang, S.-Y., Li, G., Wu, H.-B., Liu, X.-G., Yao, Y.-H., Tao, L., & Liu, H. (2011). An integrated recirculating aquaculture system (RAS) for land-based fish farming: The effects on water quality and fish production. Aquacultural Engineering, 45(3), 93–102. https://doi.org/10.1016/j.aquaeng.2011.08.001

Zhou, X., Li, D., Zhang, L., & Duan, Q. (2021). Application of an adaptive PID controller enhanced by a differential evolution algorithm for precise control of dissolved oxygen in recirculating aquaculture systems. Biosystems Engineering, 208, 186–198. https://doi.org/10.1016/j.biosystemseng.2021.05.019

Zhou, X., Wang, J., Huang, L., Li, D., & Duan, Q. (2022). Modelling and controlling dissolved oxygen in recirculating aquaculture systems based on mechanism analysis and an adaptive PID controller. Computers and Electronics in Agriculture, 192, 106583. https://doi.org/10.1016/j.compag.2021.106583

APPENDIX

A. Biological treatment: Kinetics, parameters, and stoichiometry coefficients

Table. A1 is used to calculate the rate of change of the components in the biological reactors. The biological processes taking place in the moving bed bioreactor (MBBR) is based on the zero-dimensional biofilm model (0DBFM) proposed by Plattes et al., (2008) while the nitrification process considered in the 0DBFM is adjusted based on the modifications proposed by Ostace et al., (2011). Consequently, rate of change of component i ($r_{0D\ BFM_i}$) in the biological reactors can be calculated as follows:

$$r_{0D\ BFM_i} = \sum_j v_{i,j}\rho_j \quad \text{(A1)}$$

where ρ_j represents process j (see Table A1) and $v_{i,j}$ is the corresponding stoichiometric coefficient of component i in process j (See table A2).

Table A1

Process kinetics

	Processes	Process rate equation ρ_j
1	Aerobic growth of heterotrophs in the suspension	$\mu_H \frac{S_S}{K_S + S_S} \frac{S_O}{K_{O,H} + S_O} X^S{}_{B,H}$
2	Aerobic growth of heterotrophs in the biofilm	$\mu_H \frac{S_S}{K_S + S_S} \frac{S_O}{K_{O,H} + S_O} X^B{}_{B,H}$
3	Anoxic growth of heterotrophs on S_{NO2} in the suspension	$\mu_H \eta_{NO2} \frac{S_S}{K_S + S_S} \frac{K_{O,H}}{K_{O,H} + S_O} \frac{S_{NO2}}{K_{NOx} + S_{NO2}} \frac{S_{NO2}}{S_{NO2} + S_{NO3}} X^S{}_{B,H}$
4	Anoxic growth of heterotrophs on S_{NO2} in the biofilm	$\mu_H \eta_{NO2} \frac{S_S}{K_S + S_S} \frac{K_{O,H}}{K_{O,H} + S_O} \frac{S_{NO2}}{K_{NOx} + S_{NO2}} \frac{S_{NO2}}{S_{NO2} + S_{NO3}} X^B{}_{B,H}$

5	Anoxic growth of heterotrophs on S_{NO3} in the suspension	$\mu_H \eta_{NO3} \frac{S_S}{K_S + S_S} \frac{K_{O,H}}{K_{O,H} + S_O} \frac{S_{NO3}}{K_{NOx} + S_{NO2}} \frac{S_{NO3}}{S_{NO3} + S_{NO3}} X^S{}_{B,H}$
6	Anoxic growth of heterotrophs on S_{NO3} in the biofilm	$\mu_H \eta_{NO3} \frac{S_S}{K_S + S_S} \frac{K_{O,H}}{K_{O,H} + S_O} \frac{S_{NO3}}{K_{NOx} + S_{NO2}} \frac{S_{NO3}}{S_{NO3} + S_{NO3}} X^B{}_{B,H}$
7	Decay of heterotrophs in the suspension	$b_H X^S{}_{B,H}$
8	Decay of heterotrophs in the biofilm	$b_H X^B{}_{B,H}$
9	Aerobic growth of AOB in the suspension	$\mu_{AOB} \frac{S_{NH}}{K_{NH} + S_{NH}} \frac{S_O}{K_{O,A} + S_O} X^S{}_{AOB}$
10	Aerobic growth of AOB in the biofilm	$\mu_{AOB} \frac{S_{NH}}{K_{NH} + S_{NH}} \frac{S_O}{K_{O,A} + S_O} X^B{}_{AOB}$
11	Aerobic growth of NOB in the suspension	$\mu_{NOB} \frac{S_{NO2}}{K_{NO2} + S_{NO2}} \frac{S_O}{K_{O,A} + S_O} \frac{K_{NH,I}}{K_{NH,I} + S_{NH}} X^S{}_{NOB}$
12	Aerobic growth of NOB in the suspension in the biofilm	$\mu_{NOB} \frac{S_{NO2}}{K_{NO2} + S_{NO2}} \frac{S_O}{K_{O,A} + S_O} \frac{K_{NH,I}}{K_{NH,I} + S_{NH}} X^B{}_{NOB}$
13	Decay of AOB in the suspension	$b_{AOB} X^S{}_{AOB}$
14	Decay of AOB in the biofilm	$b_{AOB} X^B{}_{AOB}$
15	Decay of NOB in the suspension	$b_{NOB} X^S{}_{NOB}$
16	Decay of NOB in the biofilm	$b_{AOB} X^B{}_{NOB}$
17	Ammonification of soluble organic nitrogen	$K_a S_{ND} (X^B{}_{B,H} + X^S{}_{B,H})$
18	Hydrolysis of entrapped organics in the suspension	$K_h \frac{X_S/X^S{}_{B,H}}{K_X + X_S/X^S{}_{B,H}} \left[\frac{S_O}{K_{O,H} + S_O} + \eta_g \frac{K_{O,H}}{K_{O,H} + S_O} \frac{S_{NO2} + S_{NO3}}{K_{NOX} + S_{NO2} + S_{NO3}} \right] X^S{}_{B,H}$
19	Hydrolysis of entrapped organics in the biofilm	$K_h \frac{X_S/X^B{}_{B,H}}{K_X + X_S/X^B{}_{B,H}} \left[\frac{S_O}{K_{O,H} + S_O} + \eta_g \frac{K_{O,H}}{K_{O,H} + S_O} \frac{S_{NO2} + S_{NO3}}{K_{NOX} + S_{NO2} + S_{NO3}} \right] X^B{}_{B,H}$

20	Hydrolysis of entrapped organic nitrogen in the suspension	$\rho_{10} \frac{X^S{}_{ND}}{X^S{}_S}$
21	Hydrolysis of entrapped organic nitrogen in the biofilm	$\rho_{10} \frac{X^B{}_{ND}}{X^B{}_S}$
22	Attachment of particulate inert organic matter	$K_a(X^S{}_I + X^S{}_S + X^S{}_{B,H} + X^S{}_{AOB} + X^S{}_{NOB} + X^S{}_P) * icv + X^S{}_{II}) * X^S{}_I$
23	Attachment of slowly biodegradable substrate	$K_a(X^S{}_I + X^S{}_S + X^S{}_{B,H} + X^S{}_{AOB} + X^S{}_{NOB} + X^S{}_P) * icv + X^S{}_{II}) * X^S{}_S$
24	Attachment of active heterotrophic biomass	$K_a(X^S{}_I + X^S{}_S + X^S{}_{B,H} + X^S{}_{AOB} + X^S{}_{NOB} + X^S{}_P) * icv + X^S{}_{II}) * X^S{}_{B,H}$
25	Attachment of active AOB	$K_a(X^S{}_I + X^S{}_S + X^S{}_{B,H} + X^S{}_{AOB} + X^S{}_{NOB} + X^S{}_P) * icv + X^S{}_{II}) * X^S{}_{AOB}$
26	Attachment of active NOB	$K_a(X^S{}_I + X^S{}_S + X^S{}_{B,H} + X^S{}_{AOB} + X^S{}_{NOB} + X^S{}_P) * icv + X^S{}_{II}) * X^S{}_{NOB}$
27	Attachment of particulate products arising from biomass decay	$K_a(X^S{}_I + X^S{}_S + X^S{}_{B,H} + X^S{}_{AOB} + X^S{}_{NOB} + X^S{}_P) * icv + X^S{}_{II}) * X^S{}_P$
28	Attachment of particulate biodegradable organic nitrogen	$K_a(X^S{}_I + X^S{}_S + X^S{}_{B,H} + X^S{}_{AOB} + X^S{}_{NOB} + X^S{}_P) * icv + X^S{}_{II}) * X^S{}_{ND}$
29	Detachment of particulate inert organic matter	$K_d(X^B{}_I + X^B{}_S + X^B{}_{B,H} + X^B{}_{AOB} + X^B{}_{NOB} + X^B{}_P) * icv + X^B{}_{II}) * X^B{}_I$
30	Detachment of slowly biodegradable substrate	$K_d(X^B{}_I + X^B{}_S + X^B{}_{B,H} + X^B{}_{AOB} + X^B{}_{NOB} + X^B{}_P) * icv + X^B{}_{II}) * X^B{}_S$
31	Detachment of active heterotrophic biomass	$K_d(X^B{}_I + X^B{}_S + X^B{}_{B,H} + X^B{}_{AOB} + X^B{}_{NOB} + X^B{}_P) * icv + X^B{}_{II}) * X^B{}_S$
32	Detachment of active AOB	$K_d(X^B{}_I + X^B{}_S + X^B{}_{B,H} + X^B{}_{AOB} + X^B{}_{NOB} + X^B{}_P) * icv + X^B{}_{II}) * X^B{}_{AOB}$
33	Detachment of active NOB	$K_d(X^B{}_I + X^B{}_S + X^B{}_{B,H} + X^B{}_{AOB} + X^B{}_{NOB} + X^B{}_P) * icv + X^B{}_{II}) * X^B{}_{AOB}$

34	Detachment of particulate products arising from biomass decay	$K_d(X^B{}_I + X^B{}_S + X^B{}_{B,H} + X^B{}_{AOB} + X^B{}_{NOB} + X^B{}_P) * icv + X^B{}_{II}) * X^B{}_P$
35	Detachment of particulate biodegradable organic nitrogen	$K_d(X^B{}_I + X^B{}_S + X^B{}_{B,H} + X^B{}_{AOB} + X^B{}_{NOB} + X^B{}_P) * icv + X^B{}_{II}) * X^B{}_{ND}$

Table A2

Process stoichiometric coefficients

	S_I	S_s	$X^s{}_I$	$X^B{}_I$	$X^S{}_S$	$X^B{}_S$	$X^S{}_{B,H}$	$X^B{}_{B,H}$	$X^S{}_{AOB}$	$X^B{}_{AOB}$	$X^S{}_{NOB}$	$X^B{}_{NOB}$	$X^S{}_P$	$X^B{}_P$	S_{NO2}	S_{NO3}	S_{NH}	S_{N}	$X^S{}_{ND}$	$X^B{}_{ND}$
1		$-\frac{1}{\gamma}$					1										$-i_{XB}$			
2		$-\frac{1}{\gamma}$						1									$-i_{XB}$			
3		$-\frac{1}{\gamma}$					1								$-\frac{1-\gamma}{1.72\gamma}$		$-i_{XB}$			
4		$-\frac{1}{\gamma}$						1							$-\frac{1-\gamma}{1.72\gamma}$		$-i_{XB}$			
5		$-\frac{1}{\gamma}$														$-\frac{1-}{2.86}$	$-i_{XB}$			
6		$-\frac{1}{\gamma}$														$-\frac{1-}{2.86}$	$-i_{XB}$			
7					1-f_p		-1						f_p						$i_{XB}-f_p i_{XP}$	
8						1-f_p		-1						f_p						$i_{XB}-f_p$
9									1						$\frac{1}{\gamma_{AOB}}$		$-i_{XB}$ $-\frac{1}{\gamma_{AO}}$			
10										1					$\frac{1}{\gamma_{AOB}}$		$-i_{XB}$ $-\frac{1}{\gamma_{AO}}$			
11											1				$-\frac{1}{\gamma_{NOB}}$	$\frac{1}{\gamma_{NOB}}$	$-i_{XB}$			

12												1			$-\frac{1}{\gamma_{NOB}}$	$\frac{1}{\gamma_{NOB}}$	$-i_{XB}$			
13					1-f_p				-1				f_p						$i_{XB}-f_p i_{XP}$	
14						1-f_p				-1				f_p						$i_{XB}-f_p$
15					1-f_p						-1		f_p						$i_{XB}-f_p i_{XP}$	
16						1-f_p						-1		f_p						$i_{XB}-f_p$
17																	1	-1		
18		1			-1															
19		1				-1														
20																		1	-1	
21																		1		-1
22			-1	1																
23					-1	1														
24							-1	1												
25									-1	1										
26											-1	1								
27													-1	1						
28																			-1	1
29			1	-1																
30					1	-1														
31							1	-1												
32									1	-1										
33											1	-1								
34													1	-1						
35																			1	-1

Table B1

Model parameters

Parameter	Description	Value	Source
a	Fraction of the food assimilated that is used for feeding catabolism	0.4	(Dampin et al., 2012)
A_{crit}	Critical unionized ammonia concentration (mg/L)	0.0125	(Timmons et al., 2002)
A_{max}	Maximum unionized ammonia concentration (mg/L)	1.4	(Dampin et al., 2012)
b_{AOB}	Decay coefficient for AOB bacteria (day^{-1})	0.05	(Ostace et al., 2011)
b_{NOB}	Decay coefficient for NOB bacteria (day^{-1})	0.05	(Ostace et al., 2011)
b_H	Decay coefficient for heterotrophic biomass (day^{-1})	0.3	(Ostace et al., 2011)
c	Allometric scaling factor	-0.605	(Lorenzen, 1996)
DO_{crit}	Critical dissolved oxygen (mg/L)	6.98	(Noble, 2020)
DO_{min}	Minimum dissolved oxygen (mg/L)	5.3	(Noble, 2020)
f	Food availability	1	
f_P	Fraction of biomass leading to particulate products (dimensionless)	0.08	(Plattes et al., 2008)
h	Coefficient of food consumption ($g^{1-m}day^{-1}$)	0.08	(Dampin et al., 2012)
i_{CV}	Particulate COD/volatile suspended solids (dimensionless)	1	(Plattes et al., 2008)
i_{XB}	Mass of nitrogen per mass of COD in biomass ($g\ N\ /\ g\ COD$)	0.08	(Ostace et al., 2011)
i_{XP}	Mass of nitrogen per mass of COD in products from biomass $g\ N\ /\ g\ COD$	0.06	(Ostace et al., 2011)
J	Constant to describe temperature on catabolism (℃$^{-1}$)	0.0132	(Dampin et al., 2012)
K	Catabolism coefficient ($g^{1-m}day^{-1}$)	Eq.19	
K_a	Ammonification rate ($m^3(gCODday)^{-1}$)	0.05	(Ostace et al., 2011)
k_{attach}	Attachment rate constant ($m^3g^{-1}day^{-1}$)	0.3	(Plattes et al., 2008)
k_{detach}	Detachment rate constant ($m^3g^{-1}day^{-1}$)	0.0009	(Plattes et al., 2008)
$K_{L,CO2}$	Mass transfer coefficient for carbon dioxide (day^{-1})	500	(Wik et al., 2009)
$K_{L,O2}$	Mass transfer coefficient for oxygen (day^{-1})	500	(Wik et al., 2009)
k_{min}	Coefficient of fasting catabolism ($g^{1-n}day^{-1}$)	0.00133	(Dampin et al., 2012)
K_{NH}	Half-saturation (auto. growth) ($(gNH_3 - Nm^{-3})$	1	(Ostace et al., 2011)
$K_{NH,I}$	Ammonia inhibition of nitrite oxidation ($gNH_4 - Nm^{-3}$)	5	(Ostace et al., 2011)
K_{OA}	Half-saturation (auto. oxygen) ((gO_2m^{-3})	0.4	(Ostace et al., 2011)
K_{OH}	Half-saturation (hetero. oxygen) ($(gNH_3 - Nm^{-3})$	0.2	(Ostace et al., 2011)
K_{NOx}	Half-saturation (nitrite and nitrate) ($gNO_3 - Nm^{-3}$)	0.5	(Ostace et al., 2011)

K_S	Half-saturation (hetero. growth) ($gCODm^{-3}$)	10	(Ostace et al., 2011)
K_X	Half-saturation (Hydrolysis)	0.1	(Ostace et al., 2011)
m	Exponent of body weight for net anabolism	0.67	(Dampin et al., 2012)
M_u	Natural mortality rate at unit weight	0.0037	(Lorenzen, 1996)
n	Exponent of body weight for fasting catabolism	0.81	(Dampin et al., 2012)
${pK_a}^0$	Ionization constant at 25℃ for the ammonium ion	9.245	(Fivelstad et al., 1995)
T_{min}	Lower limit for temperature (℃)	1	(Woynarovich, 2011)
T_{max}	Upper limit for temperature (℃)	25	(Woynarovich, 2011)
T_{opt}	Optimal temperature (℃)	16	(SCHURMANN et al., 1991)
Y_{AOB}	AOB yield ($g\ COD\ /\ g\ N$)	0.21	(Ostace et al., 2011)
Y_{NOB}	NOB yield ($g\ COD\ /\ g\ N$)	0.03	(Ostace et al., 2011)
Y_H	Heterotrophic yield ($g\ COD\ /\ g\ N$)	0.67	(Ostace et al., 2011)
ε_{loss}	Feed loss fraction	0.05	
η_g	Anoxic growth rate correction factor (dimensionless)	0.8	(Ostace et al., 2011)
η_h	Anoxic growth rate correction factor (dimensionless)	0.8	(Ostace et al., 2011)
η_{NO2}	Anoxic growth rate correction factor S_{NO2} (dimensionless)	0.8	(Ostace et al., 2011)
η_{NO3}	Anoxic growth rate correction factor S_{NO3}(dimensionless)	0.8	(Ostace et al., 2011)
μ_H	Maximum heterotrophic growth rate (day^{-1})	4	(Ostace et al., 2011)
μ_{NB}	Maximum NOB growth rate (day^{-1})	1.68	(Ostace et al., 2011)
μ_{NS}	Maximum AOB growth rate (0.5 day^{-1})	0.5	(Ostace et al., 2011)
τ	Feed residence time (day)	0.211	(Clark et al., 1985)

Table B2

Initial conditions used in Chapter 3.

Variable	Value (kg/m^3)
S_{CO2}	0.008
S_I	0.0001
S_{ND}	0.00247
S_{NH}	0.006
S_{NO2}	0.0001

S_{NO3}	0.0003
S_O	0.008
S_S	0.0004
X_{AOB}^B	0.001
X_{AOB}^S	0.001
X_{NOB}^B	0.001
X_{NOB}^S	0.001
X_H^B	0.001
X_H^S	0.001
X_I^B	0.00026
X_I^S	0.00026
X_{ND}^B	0.00121
X_{ND}^S	0.00121
X_P^B	0.0003
X_P^S	0.0003
X_S^B	0.0003
X_S^S	0.00124
W	45

Table B3

Nominal values of the states used in Chapter 4.*

Variable	Value (kg/m^3)
$S_{I,FT}$	0.025
$S_{ND,FT}$	0.0027
$S_{NH,FT}$	0.00062

$S_{NO2,FT}$	0.00028
$S_{NO3,FT}$	0.021
$S_{O,FT}$	0.008
$S_{S,FT}$	0.0015
$X^S_{AOB,FT}$	0.0033
$X^S_{NOB,FT}$	0.00047
X^S_H	0.0104
X^S_I	0.00086
X^S_{ND}	0.00062
X^S_P	3.23e-5
X^S_S	0.0013
$S_{I,BR}$	0.025
$S_{ND,BR}$	0.0026
$S_{NH,BR}$	0.00049
$S_{NO2,BR}$	0.00028
$S_{NO3,BR}$	0.021
$S_{O,BR}$	0.008
$S_{S,BR}$	0.0013
$X^B_{AOB,BR}$	0.082
$X^S_{AOB,BR}$	0.0034
$X^B_{NOB,BR}$	0.0115
$X^S_{NOB,BR}$	0.00047
$X^B_{H,BR}$	0.255
$X^S_{H,BR}$	0.0105

$X_{I,BR}^{B}$	0.0062
$X_{I,BR}^{S}$	0.00045
$X_{ND,BR}^{B}$	0.00032
$X_{ND,BR}^{S}$	0.0006
$X_{P,BR}^{B}$	0.0195
$X_{P,BR}^{S}$	3.26e-5
$X_{S,BR}^{B}$	0.0028
$X_{S,BR}^{S}$	0.00065

* Subscript *FT* represents fish tank whereas subscript *BR* indicates the biological reactor.